THESIS

NONLINEAR FREE VIBRATION OF BEAMS BY ONE-DIMENSIONAL AND ELASTICITY SOLUTIONS

Submitted by

Abdullah N. Asiri

Department of Civil and Environmental Engineering

In partial fulfillment of the requirements

For the Degree of Master of Science

Colorado State University

Fort Collins, Colorado

Fall 2018

Master's Committee:

Advisor: Paul Heyliger

Suren Chen
Mike O'Reilly

ABSTRACT

NONLINEAR FREE VIBRATION OF BEAMS BY ONE-DIMENSIONAL AND ELASTICITY SOLUTIONS

In this research, linear and nonlinear free vibration are examined. A three-dimensional rectangular parallelepiped free–free beam is studied based on the Ritz method. The equation of motion is derived depending on Hamilton's principle. A validation of the Ritz method formulation has been conducted by comparison with the Euler–Bernoulli beam theory. The impact of three-dimensional beam length has been investigated as well.

In terms of nonlinear analysis, a two-dimensional clamped–clamped beam was studied. Total Lagrange formulation is adopted for the elasticity method based on the Green–Lagrange strain tensor and second Piola–Kirchhoff stress tensor. The outcomes of the approximated method have been compared by using the nonlinear Euler–Bernoulli theory depending on the Hermite and Lagrange interpolations. The solutions of both theories are computed according to the direct iteration method. Poisson's ratio effect is studied with two assumptions, as well as the impact of the Gauss evaluations.

ACKNOWLEDGMENTS

I would like to thank every person who put forth an effort to help me in this thesis. Great gratitude and appreciation go to Paul Heyliger for giving me the honor of cooperating with him; for his support, advice, and encouragement until this work is completed. I would also like to thank committee members Suren Chen and Mike O'Reilly for their help and support.

Appreciation and great thanks to my father, my mother and each member in my family for their continuous support and prayers.

Finally, I would like to thank the Saudi government, represented by King Khaled University, for giving me the opportunity to complete my master's degree at Colorado State University and for its financial support and cooperation.

TABLE OF CONTENTS

ABSTRACT ii
ACKNOWLEDGMENTS iii
LIST OF TABLES vi
Chapter 1 – Introduction 1
1.1 Overview 1
1.2 Organization 3
Chapter 2 – Literature Review 4
2.1 Background 4
2.2 Linear Vibration 4
2.3 Nonlinear Vibration 6
2.4. Significance 12
Chapter 3 – Methodology 13
3.1 Linear Analysis 13
3.1.1 Overview 13
3.1.2 Ritz Method 13
3.1.3 Discretization 14
3.2 Elasticity Method 14
3.2.1 Ritz Approximation in Linear Analysis 15
3.3 Euler–Bernoulli Theory 17
3.3.1 Frequency of Euler–Bernoulli Beam Theory 17
3.3.2 Boundary Conditions 18
3.4 Gaussian Quadrature Evaluation 19
3.5 Nonlinear Analysis 20
3.5.1 Nonlinear Deflection in Euler–Bernoulli Theory 20
3.5.2 Elasticity Method 22
3.5.3 Ritz Method Formulation 24
3.6 Computation Method for Nonlinear Formulation 24
3.7 Poisson’s Ratio 25
3.8 Stiffness Matrix Equations 26
Chapter 4 – Results and Discussion 27
4.1 Overview 27
4.2. Linear Analysis Results 27
4.3 Nonlinear Analysis Results 33
4.3.1 Nonlinear Beam Theory 33
4.3.2 Nonlinear Elasticity Analysis 35
Chapter 5 – Conclusion 40
5.1 Concluding Remarks 40
5.2 Future Work 42
REFERENCES 43
Appendix A 47
A.1 Linear Analysis Results 47
A.2 The Effect of Various Lengths on the Linear Mode Shapes 59

A.3 The Mode Shapes of the Nonlinear Euler–Bernoulli Beam Theory 63

LIST OF TABLES

TABLE 4.1- Properties of the beam 27
TABLE 4.2- Natural frequency of Ritz method for N = 6 of a F–F beam.................................. 28
TABLE 4.3- Natural frequency of ritz method for N = 8 of A F–F beam.................................. 28
TABLE 4.4- Natural frequency of Ritz method for N = 10 of a F–F beam................................ 28
TABLE 4.5- $(\omega_{NL}/\omega_L)^2$ of a simply–simply supported beam 34
TABLE 4.6- $(\omega_{NL}/\omega_L)^2$ of a clamped–clamped beam... 34
TABLE 4.7- $(\omega_{NL}/\omega_L)^2$ of a clamped–simply supported beam 35
TABLE 4.8- Nonlinear frequency of a clamped–clamped beam of N = 4 36
TABLE 4.9- Nonlinear frequency of a clamped–clamped beam of N = 6 36
TABLE 4.10- Accuracy of the frequencies based on Gauss points and weights 37
TABLE 4.11- The linear frequency of υ = 0 and υ = 0.3 for a C–C beam.................................. 38
TABLE 4.12- The nonlinear frequency of υ = 0 and υ = 0.3 for a C–C beam............................ 38
TABLE 4.13- Comparison of $(\omega_{NL}/\omega_L)^2$ for N = 4 39
TABLE 4.14- Comparison of $(\omega_{NL}/\omega_L)^2$ for N = 6 39

TABLE A.1- Linear natural frequency of E–B theory for S–S and F–F beams (a/r = 1.0)......... 67
TABLE A.2- Nonlinear natural frequency of E–B theory for S–S and F–F beams (a/r = 1.0) ... 68
TABLE A.3- Linear natural frequency of E–B theory for C–C and C–H beams (a/r = 1.0)....... 69
TABLE A.4- Nonlinear natural frequency of E–B theory for C–C and C–H beams (a/r = 1.0) . 70
TABLE A.5- Linear natural frequency of E–B theory for S–S and F–F beams (a/r = 0.4)......... 71
TABLE A.6- Nonlinear natural frequency of E–B theory for S–S and F–F beams (a/r = 0.4) ... 72
TABLE A.7- Linear natural frequency of E–B theory for C–C and C–H beams (a/r = 0.4)....... 73
TABLE A.8- Nonlinear natural frequency of E–B theory for C–C and C–H beams (a/r = 0.4) . 74
TABLE A.9- Linear natural frequency when υ = 0 and υ = 0.3 for L = 10 and L = 4 of C–C beam.. 75
TABLE A.10- Nonlinear natural frequency when υ = 0 and υ = 0.3 for L = 10 and L = 4 of Clamped–Clamped beam (a/r = 1.0) 76
TABLE A.11- Linear natural frequency when υ = 0 and υ = 0.3 for L = 20 and L = 40 of a Clamped–Clamped beam (a/r = 1.0) 77
TABLE A.12- Nonlinear natural frequency when υ = 0 and υ = 0.3 for L = 20 and L = 40 of a Clamped–Clamped beam (a/r = 1.0) 78
TABLE A.13- Linear natural frequency when υ = 0 and υ = 0.3 for L = 10 and L = 4 of a C–C beam (a/r = 1.5) 79
TABLE A.14- Nonlinear natural frequency when υ = 0 and υ = 0.3 for L = 10 and L = 4 of a C–C beam (a/r = 1.5)... 80
TABLE A.15- Linear natural frequency when υ = 0 and υ = 0.3 for L = 20 and L = 40 of a C–C beam (a/r = 1.5) 81
TABLE A.16- Nonlinear natural frequency when υ = 0 and υ = 0.3 for L = 20 and L = 40 of a C–C beam (a/r = 1.5)... 82

TABLE A.17- Linear natural frequency when υ = 0 and υ = 0.3 for *L* = 10 and *L* = 4 of a C–C beam (*a*/*r* = 2.0) 83
TABLE A.18- Nonlinear natural frequency when υ = 0 and υ = 0.3 for *L* = 10 and *L* = 4 of a C–C beam (*a*/*r* = 2.0)........ 84
TABLE A.19- Linear natural frequency when υ = 0 and υ = 0.3 for *L* = 20 and *L* = 40 of a C–C beam (*a*/*r* = 2.0) 85
TABLE A.20- Nonlinear natural frequency when υ = 0 and υ = 0.3 for *L* = 20 and *L* = 40 of a C–C beam (*a*/*r* = 2.0)........ 86

Chapter 1 – Introduction

1.1 Overview

In recent days, studying the vibrational behavior of structures has become interesting to researchers and designers because of the critical role this phenomenon plays in failure conditions. Elements that have mass and elastic status are qualified to produce vibrational motions. To understand when vibrations can be observed, most human activities, such as speaking, running and respiration, include oscillational motion. For the safest results in design, construction, and operation of a structure, it is important to consider this kind of dynamic behavior (Rao, 2007).

In Hook's formulation, Newton's second law and differential equations help investigate the vibration of continuous systems such as strings, bars, and beams. For beam vibration, engineers and designers are concerned with studying the dynamic behavior of vibration, especially that of earthquake motion. In addition, the importance of a beam lies in its ability to represent any elements that need to be examined, such as aircraft wings, rocket missiles, or submarines. Therefore, studying the dynamic behavior of such elements' geometries is worthwhile. Consideration of these examples with no external factors such as air or water would result in linear deformation conditions. However, objects interact with air and water in nature, so the deformation conditions in this case become nonlinear (Anindya, 2009). Concentrating on beam vibration, Daniel Bernoulli studied thin beam oscillation in 1735, creating the equation of motion of transverse vibration. Euler extended this study by applying various boundary conditions which led to what is now known as Euler–Bernoulli theory, which is the beam theory adopted by this investigation as recommended by Rao (2007).

However, applying the beam theory for two- or three-dimensional problems tends to be difficult. Exact solutions provide clear ideas of the oscillations and mode shapes of simple problems, reflecting the infinite number of series that describe the normal modes of vibration. However, some vibration problems have complexity in the form of differential equations or boundary conditions; in such cases, approximate solutions would be preferable. Approximate solutions have been classified by Rao (2007) in two categories. The first category depends on a finite number of series, which involve a set of functions that is multiplied by unknown factors. The set of functions can be formulated according to the approach used. For instance, in the Ritz method, a set of functions should satisfy three conditions: (a) essential boundary conditions should be formed homogeneously; (b) they should be built in complexity, meaning functions start from the simplest form then increase in complexity; and (c) they must be linearly independent. Hence, the maximum number of series used yields corresponding numbers of eigenvalues as well as the eigenfunctions which are applied in this research.

The second category is built upon the simple lamping of system properties. The concept of this approach is, for example, to concentrate the mass of a system on specified points described as stations; the parts between these stations are called fields, and the stiffness in this case is considered uniformly distributed, neglecting the mass of these fields. This approach tends to be more conjectural in nature; the Ritz method is considered more analytical, so the latter approximation is the analytical solution used in this research.

In this research, a three dimensional free–free beam has been examined for linear vibration analysis according to the elasticity method. The elasticity method was formulated based on the Ritz approximation method with the series of polynomials in a Cartesian coordinate system. To investigate the accuracy of the analytical solution, the Euler–Bernoulli beam theory has been applied to compare its results to those of the elasticity method. The maximum number of powers related to the polynomial has been tested for 6, 8, and 10 where represented by the variables of the polynomial in x, y, and z directions with consideration of the effects of increasing them on the natural frequency as well. The aim of studying the linear vibration refers to the special case in which nonlinear vibration is generalized from the linear behavior of any structural element.

Nonlinear investigation was considered for a clamped–clamped rectangular beam. The approximation function was applied in terms of trigonometric functions instead of the polynomial function. Total Lagrange formulation was used for the nonlinear elasticity formulation, based on Green–Lagrange strain tensor and second Piola–Kirchhoff stress tensor. The nonlinearity of Euler–Bernoulli theory has been investigated using Hermite and Lagrange interpolations as shape functions in the formulation with various lengths of the beam. The objective is to compare the frequencies found by the beam theory and the elasticity method with some of the previous investigations in this field.

1.2 Organization

This research is divided into five chapters: Chapter 1 is the introduction; it describes the importance of studying vibrational behavior and the reasons for applying the approximated method. Chapter 2 is a literature review of linear and nonlinear investigations for several approximated methods. Chapter 3 presents the formulas for the beam theories and the various approximated methods. Chapter 4 discusses the results of the Ritz approximation and beam theories, as well as the observed behaviors for linear and nonlinear analyses. Chapter 5, the conclusion, summarizes the study’s remarkable results and makes suggestions for future study.

Chapter 2 – Literature Review

2.1 Background

In this chapter, previous publications that studied the vibration of continuous systems are discussed, especially those that applied approximate methods. According to Rao (2007), the history of using approximate approaches dates to 1877, when the Lord Rayleigh introduced his book on sound theory. He contributed to computations of fundamental frequency based on energy, which is now known as the Rayleigh method. Another approximate method extended from Rayleigh's method was created by Ritz (1878–1909), who applied an approximate approach to boundary value problems. In addition, Galerkin (1871–1945) introduced the weighted residual approach to the Ritz method. In complex engineering problems, researchers used to impose the simple approximate method with limited degrees of freedom. However, with the development of computers and simulation systems, investigators could formulate more complex problems with multiple degrees of freedom, leading to reduced errors and supporting the inclusion of more approximate methods in several aspects.

2.2 Linear Vibration

One of the earlier papers on linear vibrations analysis was written by Eer Nisse (1967), who introduced the vibration analysis of piezoelectric disks. He considered the elastic properties of electrical phenomena. Analysis has been applied by using variational calculations that depend on the direct approximation method. The author concluded that the approach gave accurate natural frequency and mode shape compared to approximations that were used before.

Later, Ohno (1976) developed a free vibration analysis of parallelepiped rectangular crystal that was extended from Demarest's cube resource theory. Ohno aimed to determine the elastic constant from the free vibration frequency of the olivine crystal. He compared his elasticity constant results to the data of Verma (1960) and Kunazawa and Anderson (1969).

Heyliger and Al-Jilani (1992) studied the free vibration of cylinders and spheres. They utilized the governing equations, the variational statements, and the Ritz method to compute the oscillational frequency of cylinders and spheres. The researchers considered three coordinate systems in their analysis that supported the application of their formulation to several kinds of geometries. The results possessed remarkable agreement with other approaches.

Regarding dynamical analysis for beams, Reddy (2007) used the various beam theories to formulate an analytical solution of free vibration with consideration of nonlocality. Hamilton's principle has been used to express the variational statements that develop the displacement of finite elements approach for a simply supported beam. Reddy stated that nonlocal effects play a role in decreasing the values of natural frequency.

A new Timoshenko beam model was modeled by Ma, Gao, and Reddy (2008). The investigators considered the microstructure of that model to study various dynamic responses. Couple stress and Hamilton's principle are modified to develop the formulation. In terms of free vibrations, the new model shows higher natural frequency compared with the classical model. The Poisson effect has significant impact on the natural frequency, especially when $v = 0.0$. furthermore, the authors stated that the size effect would be noticeable even when the thickness of a beam is very small.

Mesut (2010) introduced functionally graded beams with vibrating boundary conditions. The Lagrange equation was used to formulate the equations of frequencies as well as the Lagrange multipliers for boundary conditions. Aluminum and alumina were used for a beam with properties varying through its thicknesses. Mesut concluded that the two formulations used provided the same amplitude values. In addition, natural frequency increases as the slenderness ratio increases. Also, Aydogdu (2006) established the vibration analysis of cross-ply laminated beam. The investigation considered various boundary conditions: free, clamped, and simply supported.

2.3 Nonlinear Vibration

Compared to linear vibration publications, nonlinear analysis is considered a newer field of study and therefore, few publications are concerned with the nonlinear vibration of beams. One of the earlier and more comprehensive investigations of nonlinear analysis was conducted by Woinowsky-Krieger (1950), who was interested in testing the nonlinear vibration of transverse loaded supported bars. He found that axial force affects the vibrational behavior in increasing oscillation as the amplitude increases. Lewandowski (1987) established another vibrational examination of beams. The author applied the analytical solutions of free nonlinear vibrations of beams with various boundary conditions. Frequency as well as mode shape were obtained by using the Ritz approximation. Lewandowski concluded that in a simply supported beam, the accuracy of the Ritz method was noticeable in comparison to other approximations due to the smaller frequency errors obtained. He observed that when the flexibility of support is great in horizontal axis with an increase in vibrational amplitude, the frequencies also increase.

The frequency of beams and plates undergoing large-amplitude free vibration was investigated by Mei (1973). He considered a large deflection as the assumption of the nonlinear behavior. The formulations of the stiffness matrix were calculated based on Berger's approach (1955), in which the nonlinear vibration of beams is investigated as a special status of plates. The results of Mei's assumptions were in agreement with other studies. He concluded that increasing in the dimensionless amplitude led to the excitation of nonlinear behavior.

Based on large bending theory, Bhashyam and Prathap (1980) formulated the Galerkin finite-element method to study the nonlinear vibrations of one-dimensional beams. The researchers applied GFEM to avoid any confusion about the frequency values of axial and translation displacements (*u* and *w*, respectively) due to conjunction of nodal quantity. The nonlinear eigenvalue problem is computed depending on the linear eigenvalue problem, and the matrix equation is produced to become an equivalent to the nonlinear matrix by applying the weighted residual method. Bhashyam and Prathap suggested simplifying computation, especially for the errors of the axial forces or frequencies that occur with changing of mode shapes that correspond to amplitude reduce.

Previously, Rao, Raju, and Raju (1976) studied nonlinear free vibration by applying the strain-displacement relation of one-dimensional beams and plates with S–S and C–C boundary conditions. The formulations were in remarkable agreement with other studies. Researchers have also found that nonlinear behavior increases as the number of the mode shapes increase.

Stupnicka (1983) generalized the Ritz approach to determine the approximated nonlinear frequencies and mode shapes of beams with nonlinear (dynamic) boundary conditions. The idea of the generalization is to create a homogenous relationship between the Ritz method and the harmonic balance principle, then apply it to dynamic examples of beams. The authors found that the mode shape and frequency must be considered as unknown instead of randomly assumed.

To study the nonlinear vibration of several kinds of materials, Ke, Yang, and Kitipornchai (2010) examined the nonlinear free vibration of composite functionally graded carbon nanotube beams based on Timoshenko beam theory as well as von Kármán geometric nonlinearity. The eigenvalue equation is obtained by applying Ritz approximation. The investigators observed that with each increment in the total polynomial powers, the results become more accurate. As the volume fractions of carbon nanotubes increase, the linear and nonlinear oscillations also increase.

Extending the investigation of functionally graded beams, Ke, Wang, Yang, and Kitipornchai (2012) then studied the nonlinear free vibration of size-dependent microbeams. They aimed to test the material under various factors such as slenderness ratio and boundary conditions. They concluded that the linear and nonlinear frequencies increased when the thickness was identical to the length of a beam.

Marur and Prathap (2005) introduced a simplification of the finite elements model of beams based on quasi-linearization technique, eliminating in-plane displacement, and compiling both theories together. They compared the new simplifications by using variationally correct models such as Galerkin, Ritz, and Lagrange type. These simplifications show the incorrect notion about computing the correct result when they applied together. Furthermore, the investigators suggested that the variationally correct models are appropriate for nonlinear vibration problems.

In 1975, Bathe, Ramm, and Wilson introduced the comparison of Lagrange formulations (total and updated) with a NONSAP program to determine the appropriate finite-element formulation. The researchers considered large-dynamics behavior (large displacement and large strains) in the investigation. Elastic, hyperelastic, and hypoelastic materials were considered. They concluded that the differences obtained in the numerical results depend on assumptions of material behavior so that, in explicit aspects, the numerical results and theory should be identical. Later, various elastic bodies were subjected to large deflection in tests by Heyliger and Reddy (1988b), who applied updated Langrage formulation. Both linear and nonlinear problems were considered to examine the accuracy and the efficiency of this approach. The finite-element formulation mixed both approximated displacements and stresses as nodal variables which increase the stiffness matrix size and the degrees of freedom per nodes. This was due to the increase of degrees of freedom caused by the mixing procedures. Heyliger and Reddy (1988b) found good agreements for this approach in comparison with the traditional displacement formula of the Ritz method. In addition, the higher order theory has been investigated in rectangular beams to study dynamic and static analyses. To include the large deflection and rotation impacts, Heyliger and Reddy (1988a) considered the Von Karman strain in the derivation of the equation of motion as well as the Hamilton principle. For finite element approximations, the displacement fields of Higher Order Theory. were formed by using the Lagrange and Hermite interpolations. Regarding vibrational analysis, the obtained oscillations of various edge conditions showed good agreement in comparison with Timoshenko's theory and elasticity results.

Another technique presented by Wilson, Farhoomand, and Bathe (1973) provided a general solution for the dynamic behavior of structures. The authors concentrated on the errors of the discrete structure nonlinear equations. The incremental form was also applied to derive the equation of motion. At the end of this investigation, the authors suggested performing more research on this formulation, especially regarding the evaluation of matrices.

In addition, Dupuis, Hibbitt, McNamara, and Marcal (1971) introduced the Eulerian approach to investigate the nonlinearity of shell structure, taking into consideration the impact of small displacements as well as initial stress. This study also formulated equations by combining the Eulerian and Lagrange approaches. They believed that this newly introduced approach yielded good indicators for consideration in nonlinear analysis.

Hibbitt, Marcal, and Rice (1970) developed linear finite-analysis theory depending on large-displacement and large-strain assumptions. This study's incremental stiffness equation was derived using the Lagrange methodology. Significantly, the formulation of finite strain has an identical level of difficulty as the current small-strain, large-rotation approximation.

Recently, a nonlinear vibration analysis approach for beams was introduced by Shen (2011), which depends on the two-step perturbation method. This method considers the small perturbation factor as having no physical impact; therefore, this factor would be ill-treated by dimensionless deflection. The nonlinear frequencies have been investigated with and without consideration of the initial stress, as well as with movable and immovable boundary conditions. Regardless of foundation type, the study admitted that the boundary conditions affect the nonlinear vibrational behavior for the Euler–Bernoulli theory.

Shen and Xiang (2013) extended the analysis of nanotube-reinforced composite beams resting on an elastic foundation. The researchers studied a case of uniform distribution and functionally graded material. The nonlinear vibration in this investigation was applied by two-step perturbation method depending on thermal bending stress and displacement fields.

On the other hand, Kitipornchai, Ke, Yang, and Xiang (2009) applied nonlinear vibration to the cracked edges of Timoshenko beams. The Ritz method and the direct iterative approach were considered to derive the nonlinear frequency and mode shape. The authors set this beam in two states, (a) intact and (b) cracked, observing that when they occur at the center of the beam, the frequency is extremely affected by the cracks. Nonlinear behavior increases as vibrational amplitude increases.

An investigation of nonlinear free vibration of orthotropic Euler–Bernoulli beam theory was conducted by Ghasemi, Taheri-Behrooz, Farahani, and Mohandes (2016). This study depended on finite strain assumption with consideration of the second Piola–Kirchhoff stress tensor and Green–Lagrange strain tensor. The contrast of linear and nonlinear mode shapes was notable in the simply supported beam condition.

Testing nonlinear vibration of beams with various aspects, Hamdan and Shabaneh (1997) applied a lumped mass in the center of beam, but its rotary inertia and shear deformation were neglected. They used Hamilton's principle and single-mode Langrage method, which neglected the condition of inextensibility. In the second approach, the authors assumed nonlinear frequencies to be the same as linear ones, expanding space and mode shapes. The results show that large errors occurred with the increase of the ratio of attached mass. The researchers also observed that similar behaviors for both linear and nonlinear vibrations occurred, especially regarding the stiffness of the base and the position and magnitude of attached mass at the small amplitudes.

Regarding sandwich beams, Kiani and Mirzaei (2016) studied the free vibration caused by temperature changes on sandwich beam with carbon-nanotube-reinforced faces. The carbon nanotubes' faces were studied in both uniformly distributed and functionally graded conditions based on Timoshenko's theory. Nonlinear formulation was derived dependent on linear derivations (Hamilton's principle). The investigators found, in general, that the nonlinear-to-linear frequency ratio increased as the temperature increased. In addition, this ratio leads the uniformly distributed beam to yield values higher than the functionally graded one. Chen, Kitipornchai, and Yang (2016) also extended the dynamic investigation of sandwich beam with consideration of both functionally graded and uniformly porous cores with three distribution forms. The researchers applied a nonlinear formulation based on Von Karman and Ritz approaches. The study showed an inverse relationship between the effects of the porosity coefficient and the nonlinear oscillation size.

A rotor-crafted blade was idealized and represented as a rotating beam to study dynamic nonlinear behavior based on the finite-element model. To achieve accurate results despite inaccuracy caused by the interfaces of various displacement components with a large number of degree-of-freedom points, Apiwattanalunggarn, Shaw, Pierre, and Jiang (2003) introduced the Galerkin and collocation-based invariant manifold approaches that led to reduced modal order for the nonlinear finite-element method.

2.4. Significance

In this investigation, the elasticity method functions as an approximated method represented by the Ritz approach to examine the dynamical behavior of the beams. Various boundary conditions are taken into consideration as well as two models. The effect of Poisson's ratio is studied for the nonlinear natural frequency. Both linear and nonlinear analyses include the impact of the various lengths of the studied beams on natural frequency and mode shapes. The approximated method results are then compared with the one-dimensional Euler–Bernoulli theory. Generally, the contribution of this work to the field is involving the nonlinear two-dimensional beam model of the elasticity method.

Chapter 3 – Methodology

In this section, linear analysis is considered the benchmark for nonlinear analysis. Both linear and nonlinear analysis formulations are discussed.

3.1 Linear Analysis

3.1.1 Overview

Linear analysis is considered the basis of nonlinear formulation. Hence, linear vibration analysis is described as the Fortran language program in terms of elasticity theory dependent on stress and strain components. This constitutive relationship is the starting point of vibration analysis. Because a simple vibrational system is an exchange between potential and kinetic energies, the Hamilton principle is applied; therefore, it is an appropriate approach for discrete dynamical problems. The Ritz method is used in addition to the displacement-strain relationship to compute the approximate solution of the weak form that leads to generalization of the eigenvalue problem. Euler–Bernoulli beam theory is applied to compare the analytical solution with the elasticity method analysis.

3.1.2 Ritz Method

Difficult geometries and boundary conditions lead the investigators to apply approximated methods in order to study the desired phenomena. The Ritz method is one of the approximation approaches that is an extension of the Rayleigh approach. The concept of the Ritz method is that the deformation of a continuous system can be evaluated over a domain using a trial function that should satisfy some conditions to be applicable. The Formulation section of this chapter describes the Ritz approximation method broadly.

3.1.3 Discretization

In this research, in order to visualize the deformed shapes, the parallelepiped beam was divided into 640 hexahedrons with eight nodes per element. This is another type of three-dimensional discretization beside the tetrahedron and wedge models. Each node was represented by three displacement components in a Cartesian coordinate system: (a) axial displacement [U]; (b) out-of-plane displacement [V]; and (c) transverse displacement [W] in the x, y, and z directions, respectively. These enabled visualization of the deformed shapes of the beam that describe the dynamical behavior. As the number of elements increase, greater accuracy of results may be obtained. SAP 2000 software has been used for the discretization process; MATLAB code visualized the final form of the hexahedron elements.

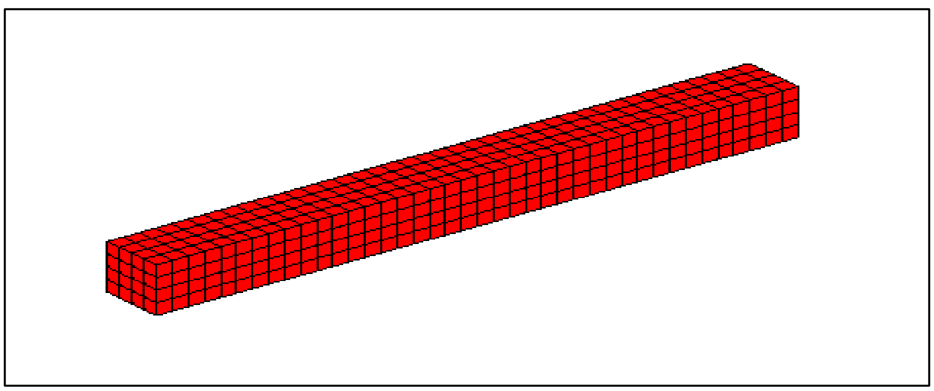

Figure 3.1 Discrete parallelepiped beam visualized by MATLAB software

3.2 Elasticity Method

The governing equations for linear free vibration are derived depending on energy relations. Lagrange equations are described as the integration of the difference of kinetic energy and potential energy with respect to the tested volume. Equation (3.1) represents the Lagrange equation as

$$L = \int_V (KE - PE)\, dV, \tag{3.1}$$

where the kinetic energy and potential energy are described as

$$KE = \frac{1}{2}\rho\omega^2 u_i u_i \tag{3.2}$$

$$PE = \frac{1}{2}C_{ijkl}u_{i,j}u_{k,l} \tag{3.3}$$

and the general constitutive relation considered in linear free vibration is

$$\begin{bmatrix}\sigma_{11}\\ \sigma_{22}\\ \sigma_{33}\\ \sigma_{23}\\ \sigma_{13}\\ \sigma_{12}\end{bmatrix} = \begin{bmatrix} C_{11} & C_{12} & C_{13} & 0 & 0 & 0\\ C_{21} & C_{22} & C_{23} & 0 & 0 & 0\\ C_{31} & C_{32} & C_{33} & 0 & 0 & 0\\ 0 & 0 & 0 & C_{44} & 0 & 0\\ 0 & 0 & 0 & 0 & C_{55} & 0\\ 0 & 0 & 0 & 0 & 0 & C_{66}\end{bmatrix}\begin{bmatrix}\varepsilon_{11}\\ \varepsilon_{22}\\ \varepsilon_{33}\\ \gamma_{23}\\ \gamma_{13}\\ \gamma_{12}\end{bmatrix}, \tag{3.4}$$

where σ_{ij} is the stress component, C_{ijkl} is the elastic stiffness tensor, and ε and γ are the normal and shear deformation the material is subjected to. The stress–strain relationship is the baseline of the free-vibration problems.3.2.1 Ritz Approximation in the Linear Analysis

The Ritz method was used to compute the approximated solutions for the displacement vectors. According to Euler–Bernoulli theory, the displacement field is introduced in Equation (3.11). According to Visscher et al. (2008), the simplest form with which to evaluate the displacement vector is the power series formulation. The function is applied depending on the Cartesian coordinate system as:

$$\phi_\lambda = x^l y^m z^n, \tag{3.5}$$

where $\lambda = (l, m, n)$ are the nonnegative integers. The powers of the polynomial function should be controlled by the following condition as:

$$l + m + n \le N \tag{3.6}$$

N here is the allowed maximum number of polynomial function. In this research, *N* of 6, 8, and 10 has been applied. The Ritz approximation has been formulated as

$$u(x) = \phi_0 + \sum_{i=1}^{n} a * \phi_\lambda(x)$$

$$v(x) \ = \ \phi_0 + \sum_{i\,=\,1}^{n} b * \phi_\lambda(x)$$

$$w(x) \ = \ \phi_0 + \textstyle\sum_{i\,=\,1}^{n} c * \phi_\lambda(x), \tag{3.7}$$

where ϕ_0 refers to the sample's natural boundary condition status; a, b, and c are the variational statement; and n is the maximum number of the functions. In Ritz approximation, the boundary condition is considered in the variational statement; therefore, ϕ_0 has been set zero, as there is no need to apply this term in that approximation. For the remaining functions, the homogeneity of the essential boundary condition and the independence of the linear condition must be satisfied according to Heyliger and Jilani (1992). Hence, $u(x), v(x)$, and $w(x)$ are the displacement fields in the *x*, *y*, and *z* directions, respectively.

Deriving the weak form refers to the stress–strain relation represented in Equation (3.4). Hence, the strain-displacement is expressed as:

$$\varepsilon_{11} \ = \ \frac{\partial U}{\partial x}, \qquad \varepsilon_{22} \ = \ \frac{\partial V}{\partial y}, \qquad \varepsilon_{33} \ = \ \frac{\partial W}{\partial z}$$

$$\gamma_{23} \ = \ \frac{\partial V}{\partial z} + \frac{\partial W}{\partial y}, \qquad \gamma_{13} \ = \ \frac{\partial U}{\partial z} + \frac{\partial W}{\partial x}, \qquad \gamma_{12} \ = \ \frac{\partial V}{\partial x} + \frac{\partial U}{\partial y} \tag{3.8}$$

Hamilton's principle can be obtained from Equation (3.4) as:

$$0 \ = \ -\int_0^t \int_V \{\sigma_1 \delta\varepsilon_1 + \sigma_2 \delta\varepsilon_2 + \sigma_3 \delta\varepsilon_3 + \sigma_4 \delta\varepsilon_4 + \sigma_5 \delta\varepsilon_5 + \sigma_6 \delta\varepsilon_6\} dV \, dt$$

$$+ \tfrac{1}{2}\delta \textstyle\int_0^t \int_V \rho(\dot{U} + \dot{V^2} + \dot{W^2}) dV \, dt \tag{3.9}$$

Substitute Equation (3.8) into the Hamilton's principle formula. Hence, the weak form will be:

$$\partial U \ = \ \int_V \Big[\left(C_{11} \frac{\partial U}{\partial x} + C_{12} \frac{\partial V}{\partial y} + C_{13} \frac{\partial W}{\partial z} \right) \frac{\partial \delta U}{\partial x} + \left(C_{12} \frac{\partial U}{\partial x} + C_{22} \frac{\partial V}{\partial y} + C_{23} \frac{\partial W}{\partial z} \right) \frac{\partial \delta V}{\partial y} +$$

$$\left(C_{13} \frac{\partial U}{\partial x} + C_{23} \frac{\partial V}{\partial y} + C_{33} \frac{\partial W}{\partial z} \right) \frac{\partial \delta W}{\partial z} + C_{44} \left(\frac{\partial V}{\partial z} + \frac{\partial W}{\partial y} \right) \left(\frac{\partial \delta W}{\partial z} + \frac{\partial \delta V}{\partial y} \right) +$$

$$C_{55}\left(\frac{\partial U}{\partial z}+\frac{\partial W}{\partial x}\right)\left(\frac{\partial \delta U}{\partial z}+\frac{\partial \delta W}{\partial x}\right)+C_{66}\left(\frac{\partial U}{\partial y}+\frac{\partial V}{\partial x}\right)\left(\frac{\partial \delta U}{\partial y}+\frac{\partial \delta V}{\partial x}\right)-$$

$$\rho\omega^2(U\delta U+V\delta V+W\delta W)\Big]\,dV \tag{3.10}$$

Now, apply the Ritz approximation and the values of the variation statements to the weak form.

The generalized eigenvalue problem is given as:

$$\begin{bmatrix} K^{11} & K^{12} & K^{13} \\ K^{21} & K^{22} & K^{23} \\ K^{31} & K^{32} & K^{33} \end{bmatrix}\begin{bmatrix} a \\ b \\ d \end{bmatrix} = \rho\omega^2\begin{bmatrix} M^{11} & 0 & 0 \\ 0 & M^{22} & 0 \\ 0 & 0 & M^{33} \end{bmatrix}\begin{bmatrix} a \\ b \\ d \end{bmatrix} \tag{3.11}$$

The mode shape of the linear elasticity method is computed using the following formulations:

$$u = \sum_{i=1}^{N} a * \phi_\lambda(x) \qquad v = \sum_{i=1}^{N} b * \phi_\lambda(x) \qquad w = \sum_{i=1}^{N} d * \phi_\lambda(x), \tag{3.12}$$

where $a, b\ and\ c$ are the eigenvectors related to the model's nodal value; u, v, and w describe the displacements on the three directions, respectively; and N is the maximum nth function in the x, y, and z directions.

3.3 Euler–Bernoulli Theory

The studied beam is considered to be a thin beam, so Euler–Bernoulli theory was applied to derive the equation of motion and the boundary conditions. In Euler–Bernoulli theory, the translations' displacements are taken into consideration, and the rotation of the cross-section is neglected, which means that the cross-section of the beams sustain the plane, normal to the centerline after bending. Hence, the displacements filed can be introduced as:

$$u = -z\frac{\partial w(x,t)}{\partial x} \qquad v = 0, \qquad w = w(x,t), \tag{3.13}$$

where u, v, and w are the displacements in the x, y, and z directions, respectively. In this research the Euler–Bernoulli theory was used for comparison with the Ritz method's results.

3.3.1 Frequency of Euler–Bernoulli Beam Theory

Based on Euler–Bernoulli theory, the solution of a free-vibration beam is:

$$W(x) = C_1 \sin\beta x + C_2 \cos\beta x + C_3 \sinh\beta x + C_4 \cosh\beta x \tag{3.14}$$

The values C_1 through C_4 are the integration constants, and sinh and cosh represent the hyperbolic triangular functions. The natural frequency is computed from:

$$\omega = \beta_{nl}^2 \sqrt{\frac{EI}{\rho A L^2}} \tag{3.15}$$

3.3.2 Boundary Conditions

This section describes the boundary conditions of this research. Free–free ends are applied to both sides of a parallelepiped rectangular beam.

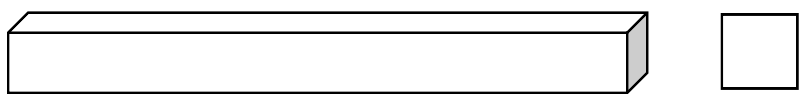

Figure 3.2: Free–free parallelepiped beam cross-section

Thus, the boundary conditions need to be defined mathematically. Each type of boundary condition has a mathematical form used to find the frequency of the desired sample. This satisfies the bending moment and shear force at the free end, so the boundary conditions of the free–free ends are:

$$EI \frac{d^2W(0)}{dx^2} = 0 \text{ or } \frac{d^2W(0)}{dx^2} = 0 \tag{3.16a}$$

$$EI \frac{d^3W(0)}{dx^3} = 0 \text{ or } \frac{d^3W(0)}{dx^3} = 0 \tag{3.16b}$$

$$EI \frac{d^2W(l)}{dx^2} = 0 \text{ or } \frac{d^2W(0)}{dx^2} = 0 \tag{3.16c}$$

$$EI \frac{d^3W(l)}{dx^3} = 0 \text{ or } \frac{d^3W(l)}{dx^3} = 0, \tag{3.16d}$$

where $W(x)$ is the differential equation of the free vibration for the beam, which is described in Equation (3.14).

After applying the operations of the boundary conditions, it is obtained as:

$$\frac{d^2W(x)}{dx^2} = \beta^2[C_1(-\cos\beta x + \cosh\beta x) + C_2(-\cos\beta x - \cosh\beta x) + C_3(-\sin\beta x + \sinh\beta x) + C_4(-\sin\beta x - \sinh\beta x)] \quad (3.17)$$

$$\frac{d^3W(x)}{dx^3} = \beta^3[C_1(\sin\beta x + \sinh\beta x) + C_2(\sin\beta x - \sinh\beta x) + C_3(-\cos\beta x + \cosh\beta x) + C_4(-\cos\beta x - \cosh\beta x)] \quad (3.18)$$

From Equations (3.16a and b), we found:

$$C_2 = C_4 = 0.0 \quad (3.19)$$

Thus, Equations (3.16c and d) gave:

$$C_1(-\cos\beta l + \cosh\beta l) + C_3(-sin\,\beta l + sinh\,\beta l) = 0 \quad (3.20)$$

$$C_1(\sin\beta l + \sinh\beta l) + C_3(-cos\,\beta l + cosh\,\beta l) = 0 \quad (3.21)$$

From Equations (3.20) and (3.21), the solutions of $C_1$and C_3 were:

$$\begin{vmatrix} -cos\,\beta l + cosh\,\beta l & -sin\,\beta l + sinh\,\beta l \\ sin\,\beta l + sinh\,\beta l & -cos\,\beta l + cosh\,\beta l \end{vmatrix} = 0 \quad (3.22)$$

In the case of a free–free end, the shape's symmetry will give an advantage by reducing the determinant's complexity. This will generate two order determinants instead of four. To reach this, the origin of the coordinate system should be placed at the center of the rectangular parallelepiped beam. The *n*th mode pattern of free–free ends beams is:

$$W_n(x) = (cos\beta_n x + \cosh\beta_n x) - \frac{\cos\beta_n l - cosh\beta_n l}{sin\beta_n l - \sinh\beta_n l}(sin\beta_n x + sinh\beta_n x) \quad (3.23)$$

3.4 Gaussian Quadrature Evaluation

Hamilton's principle was evaluated using the Gaussian quadrature method. The aim was to prepare for the nonlinear analysis, which is the goal of the project. Furthermore, it provides efficiency to the integration of the polynomial function. Gaussian quadrature is used for evaluating both stiffness and mass matrices; therefore, the Gaussian points and weights were considered in the programming process. In the Ritz method, the Gaussian quadrature evaluation occurs in parent space instead of in Cartesian coordinates. The parent space domain in a one-dimensional problem is from -1 to 1; however, in a three-dimensional problem, the domain is counted in the three directions of the parent space (ξ, η, ζ). This analysis was performed in the Fortran computing program using the coded Ritz method and Euler–Bernoulli analysis.

3.5 Nonlinear Analysis

3.5.1 Nonlinear Deflection of Euler–Bernoulli Theory

In this research, the nonlinearity of Euler–Bernoulli beams was applied for use in comparison with the outcomes of the elasticity analysis. Nonlinear analysis has different assumptions from the linear procedure. The one-dimensional bending deflection of the Euler–Bernoulli theory of linear assumption is expressed as:

$$\frac{\partial^2}{\partial x^2}\left(EI\,\frac{\partial^2 w}{\partial x^2}\right) - f \;=\; 0, \tag{3.24}$$

where $\frac{\partial^2 w}{dx^2}$ is the slope of the cross-section in the bending condition, which is assumed to be less than 1.0 in the linear analysis. However, according to Reddy (2006), concerning the nonlinear deformation, the slope is assumed to be large, and the impact of axial force the governing equation of Euler–Bernoulli in the large deflection is described as:

$$-\frac{\partial}{\partial x}\left\{EA\,\left[\frac{\partial u}{\partial x} + \frac{1}{2}\left(\frac{\partial w}{\partial x}\right)^2\right]\right\} - q \;=\; 0$$

$$\frac{\partial^2}{\partial x^2}(EI\,\frac{\partial^2 w}{\partial x^2}) - \frac{\partial}{\partial x}\left\{EA\,\frac{\partial w}{\partial x}\left[\frac{\partial u}{\partial x} + \frac{1}{2}\left(\frac{\partial w}{\partial x}\right)^2\right]\right\} - f \;=\; 0, \tag{3.25}$$

where u is the axial displacement, w is the transverse bending, E is the modulus of elasticity, and f is the transverse loading. Because the research concerns a free vibration model, the transverse loading here is 0 ($f = 0$). The weak form was found by using integration by parts in Equation (3.25), which becomes:

$$0 = \int_{x_p}^{x_q} \left\{ EA \left[\frac{\partial u}{\partial x} + \frac{1}{2} \left(\frac{\partial w}{\partial x} \right)^2 \right] - v_2 q \right\} dx - Q_1^e v_1(x_p) - Q_4^e v_1(x_q) \qquad (3.26a)$$

$$0 = \int_{x_p}^{x_q} \left\{ EI \frac{d^2 v_2}{dx^2} \frac{d^2 w}{dx^2} + EA \frac{dv_2}{dx} \frac{dw}{dx} \left[\frac{\partial u}{\partial x} + \frac{1}{2} \left(\frac{\partial w}{\partial x} \right)^2 \right] - v_2 f \right\}$$

$$-Q_2^e v_2(x_p) - Q_3^e \left(-\frac{dv_2}{dx}\right)\Big|_{x_p} - Q_2^e v_2(x_q) - Q_6^e \left(-\frac{dv_2}{dx}\right)\Big|_{x_q} \qquad (3.26b)$$

The finite-element approximations of the Euler–Bernoulli theory variables, u, w, and $-\frac{\partial w}{\partial x}$, are introduced as:

$$u = \sum_{j=1}^{n} u_j \psi_j(x) \qquad w = \sum_{j=1}^{m} s_j \phi_j(x), \qquad (3.27)$$

where u and w are the Lagrange and Hermite interpolations, respectively. By applying Equation (3.27) to (3.26), the finite-element formulation can be shown to be:

$$\begin{bmatrix} [K^{11}] & [K^{12}] \\ [K^{21}] & [K^{22}] \end{bmatrix} \begin{bmatrix} u \\ s \end{bmatrix} = 0, \qquad (3.28)$$

and

$$K_{ij}^{11} = \int_{x_p}^{x_q} EA \frac{d\psi_i}{dx} \frac{d\psi_j}{dx} \, dx$$

$$K_{ij}^{12} = \int_{x_p}^{x_q} \frac{1}{2} EA \frac{dw}{dx} \frac{d\psi_i}{dx} \frac{d\phi_j}{dx} \, dx$$

$$K_{ij}^{21} = \int_{x_p}^{x_q} EA \frac{dw}{dx} \frac{d\phi_j}{dx} \frac{d\psi_i}{dx} \, dx$$

$$K_{ij}^{22} = \int_{x_p}^{x_q} EI \frac{d^2\phi_i}{dx^2} \frac{d^2\phi_j}{dx^2} dx + \int_{x_p}^{x_q} \frac{1}{2} EA \left(\frac{dw}{dx}\right)^2 \frac{d\phi_i}{dx} \frac{d\phi_j}{dx} \, dx \qquad (3.29)$$

The linear stiffness matrix cannot be neglected in the computational procedures, as the linear vibration is the initial status of the nonlinear phenomena. The stiffness and mass matrix are taken as described in Equations (3.30a and b):

$$K = \begin{bmatrix} \frac{EA}{L} & 0 & 0 & \frac{-EA}{L} & 0 & 0 \\ 0 & \frac{12EI}{L^3} & \frac{6EI}{L^2} & 0 & \frac{-12EI}{L^3} & \frac{6EI}{L^2} \\ 0 & \frac{6EI}{L^2} & \frac{4EI}{L} & 0 & \frac{-6EI}{L^2} & \frac{2EI}{L} \\ \frac{-EA}{L} & 0 & 0 & \frac{EA}{L} & 0 & 0 \\ 0 & \frac{-12EI}{L^3} & \frac{-6EI}{L^2} & 0 & \frac{12EI}{L^3} & \frac{-6EI}{L^2} \\ 0 & \frac{6EI}{L^2} & \frac{2EI}{L} & 0 & \frac{-6EI}{L^2} & \frac{4EI}{L} \end{bmatrix} \tag{3.30a}$$

$$M = \frac{\rho AL}{420}\begin{bmatrix} 140 & 0 & 0 & 70 & 0 & 0 \\ 0 & 156 & 22L & 0 & 54 & -13L \\ 0 & 22L & 4L^2 & 0 & 13L & -3L^2 \\ 70 & 0 & 0 & 140 & 0 & 0 \\ 0 & 54 & 13L & 0 & 156 & 22L \\ 0 & -13L & -3L^2 & 0 & 22L & 4L^2 \end{bmatrix} \tag{3.30b}$$

3.5.2 Elasticity Method

The linear analysis was extended to consider the large deformation assumption. The total Lagrange formulation, introduced in the literature review, was applied to investigate the model's nonlinear behavior. The total Lagrange formulation is described by considering the motion of the body in the Cartesian coordinate system for various configurations at times 0, t, and $t + \Delta t$, which are represented in the following equations as 0, 1, and 2, respectively. In addition, the target configuration of the computational procedures is at time $t + \Delta t$, and the computation was applied with respect to the initial configuration at time 0 as well as the derivatives and integrals. The benchmark equation of this approach can be expressed as:

$$\int_V \tau^{t + \Delta t}\, \delta_{t + \Delta t}\epsilon_{ij}\, dV = {}^2\mathcal{R}, \tag{3.31}$$

which represents the principle of virtual work, with ${}^2\mathcal{R}$ representing the external virtual work. However, this equation tends to be applied to small displacements. Nonlinearity concerns problems that undergo large deformation. Thereby, Equation (3.31) can be written as:

$$\int_V {}_0^2S_{ij}\, \delta_0^2\epsilon_{ij}\, d^0V, \tag{3.32}$$

where ${}^{t+\Delta t}_{0}S_{ij}$ is the second Piola–Kirchhoff stress tensor of configuration $t + \Delta t$; this is computed with respect to the initial configuration ($t = 0$). Depending on the constitutive relations in the total Lagrange formulation, the stress–strain relations of elastic materials are given as:

$$ {}_0^2S_{ij} \;=\; {}_0C_{ijkl}\,{}_0^2\epsilon_{ij} \tag{3.33}$$

Here, ${}_0^2\epsilon_{ij}$ is the Green–Lagrange strain. It can be expressed in terms of total displacements u_i in the two directions of x_i as:

$$ {}_0^2\epsilon_{ij} \;=\; \frac{1}{2}\left(\frac{\partial_0^2 u_i}{\partial^0 x_j} + \frac{\partial_0^2 u_j}{\partial^0 x_i} + \frac{\partial_0^2 u_m}{\partial^0 x_i}\frac{\partial_0^2 u_m}{\partial^0 x_j}\right) \tag{3.34}$$

The need to increase the second Piola–Kirchhoff stresses and Green–Lagrange strain through the configurations can be shown as:

$$ {}_0^2S_{ij} \;=\; {}_0^1S_{ij} + {}_0S_{ij}$$

$$ {}_0^2\epsilon_{ij} \;=\; {}_0^1\epsilon_{ij} + {}_0\epsilon_{ij}, \tag{3.35}$$

where the ${}_0^1S_{ij}$ and ${}_0^1\epsilon_{ij}$ are the known stress and strain components, respectively. According to the definition of displacement based on the Green–Lagrange strain tensor, Equation (3.34) is referred to as the linear component, and the nonlinear incremental displacements can be expressed as:

$$ {}_0\eta_{ij} \;=\; \frac{1}{2}\; {}_0u_{k,i}\; {}_0u_{k,j} \tag{3.36}$$

The assumption of the total Lagrange formulation is that the strain ${}_0\epsilon_{ij}$ at configuration 0 is fixed through the motion of body until the configuration at $t + \Delta t$, as follows:

$$ \delta^{t+\Delta t}\; {}_0\epsilon_{ij} \;=\; \delta\; {}_0\epsilon_{ij} \tag{3.37}$$

Equation (3.33) involves the relation between the stiffness tensor and the Green–Lagrange strain. Thereby, the virtual work equation is:

$$\int_V {}_0C_{ijkl}\ {}_0\epsilon_{kl}\, \delta_0\epsilon_{ij}\ d^0V + \int_V {}_0^1S_{ij}\, \delta_0\ \eta_{ij}\ d^0V \ = \ {}^2\mathcal{R} - \int_V {}_0^1S_{ij}\, \delta_0\ \epsilon_{ij}\ d^0V, \qquad (3.38)$$

where the right-hand side includes the known displacements, and the unknown components are represented on the left side. This equation will be evaluated via Ritz approximation.

3.5.3 Ritz Method Formulation

The displacement components of the two-dimensional model are described as:

$$u \ = \ \sum_{j\,=\,1}^{n} u_j {\psi_j}^u$$

$$w \ = \ \sum_{j\,=\,1}^{n} w_j {\psi_j}^w, \qquad (3.39)$$

with the axial and transverse displacements being the investigated components in this case. The shape function ψ_j in the nonlinear analysis is expressed as:

$$\psi_j \ = \ sin\frac{n\pi x}{l} z^n, \qquad (3.40)$$

where n, the maximum number of the shape function, is controlled by the conditions of Equation (3.6). After evaluating these approximations in Equation (3.38), the weak form becomes:

$$({}_0^tK_L + {}_0^tK_{NL})u \ = \ R^{t+\Delta t}, \qquad (3.41)$$

where ${}_0^tK_L$ and ${}_0^tK_{NL}$ are the linear and nonlinear stiffness, which are provided in Section 3.8.

3.6 Computation Method for Nonlinear Formulation

To compute the assembled nonlinear equations from Equation (3.28), the approximate solution should be applied. The direct iterative method is recommended for the nonlinear formulations. The concept of this method is based on the solution of multiple iterations—the coefficients K_{ij} introduced in Equation (3.29) are the obtained solutions of the previous iteration. Equation (3.42) describes the concept as:

$$[K(\{\Delta\}^r)]\{\Delta\}^{r+1} \ = \ \{F\}, \qquad (3.42)$$

where $\{\Delta\}^r$ is the solution of the iteration (r). Therefore, the solutions of the coefficients K_{ij} are computed as:

$$\{\Delta\}^{r+1} = \frac{\{F\}}{[K(\{\Delta\}^r)]} \tag{3.43}$$

In the initial iteration—for example, $r = 0$—the solution will be assumed as $\{\Delta\}^0 = \{0\}$. This yields a redaction of the nonlinear stiffness matrix to be treated as a linear matrix. Thereby, Equation (3.43) produces a linear solution for the equations. The process will be repeated for every iteration until the errors are reduced. This approach was applied to the computational code for both the beam theory analysis and elasticity method.

3.7 Poisson's Ratio

The impact of Poisson's ratio on the dynamical behavior was considered. The objective of this investigation is to evaluate the elastic constants' contribution if the Poisson's ratio changes. Poisson's ratio is the amount of transverse strains divided by the axial strains. Usually in this assumption, the extended directions are perpendicular to the compressed directions. Poisson's ratio impacts the elastic constants. The relationships between Poisson's ratio and the module of elasticity (E) and shear module (G) are expressed as:

$$G = \frac{E}{2(1+\upsilon)}, \tag{3.44}$$

where υ is Poisson's ratio. For the isotropic material, the components of the elastic stiffness tensor regarding Poisson's ratio are given as:

$$C_{11} = C_{22} = C_{33} = \frac{E(\upsilon-1)}{(\upsilon+1)(2\upsilon-1)} \tag{3.45}$$

$$C_{12} = C_{13} = C_{23} = -\frac{E\upsilon}{(\upsilon+1)(2\upsilon-1)} \tag{3.46}$$

$$C_{44} = C_{55} = C_{66} = \frac{1}{G} \tag{3.47}$$

The elastic stiffness matrix is described as:

$$\begin{bmatrix} \frac{E(v-1)}{(v+1)(2v-1)} & -\frac{Ev}{(v+1)(2v-1)} & -\frac{Ev}{(v+1)(2v-1)} & 0 & 0 & 0 \\ -\frac{Ev}{(v+1)(2v-1)} & \frac{E(v-1)}{(v+1)(2v-1)} & -\frac{Ev}{(v+1)(2v-1)} & 0 & 0 & 0 \\ -\frac{Ev}{(v+1)(2v-1)} & -\frac{Ev}{(v+1)(2v-1)} & \frac{E(v-1)}{(v+1)(2v-1)} & 0 & 0 & 0 \\ 0 & 0 & 0 & \frac{1}{G} & 0 & 0 \\ 0 & 0 & 0 & 0 & \frac{1}{G} & 0 \\ 0 & 0 & 0 & 0 & 0 & \frac{1}{G} \end{bmatrix} \tag{3.48}$$

3.8 Stiffness Matrix Equations

$${}_{l}^{1}K_{ij}^{13} = \int_V (C_{13}\frac{\partial\psi_i^u}{\partial x}\frac{\partial\psi_j^w}{\partial z} + C_{55}\frac{\partial\psi_i^u}{\partial z}\frac{\partial\psi_i^w}{\partial x})\, dV$$

$${}_{nl}^{2}K_{ij}^{13} = \int_V [C_{11}\frac{\partial\psi_i^u}{\partial x}\frac{\partial\psi_j^w}{\partial x}\left(\frac{1}{2}\frac{\partial w}{\partial x}\right)]\, dV$$

$${}_{l}^{1}K_{ij}^{33} = \int_V (C_{33}\frac{\partial\psi_i^w}{\partial z}\frac{\partial\psi_j^w}{\partial z} + C_{44}\frac{\partial\psi_i^w}{\partial y}\frac{\partial\psi_i^w}{\partial y} + C_{55}\frac{\partial\psi_i^w}{\partial x}\frac{\partial\psi_i^w}{\partial x})\, dV$$

$${}_{nl}^{2}K_{ij}^{33} = \int_V [C_{13}\frac{\partial\psi_i^w}{\partial z}\frac{\partial\psi_j^w}{\partial x}\left(\frac{1}{2}\frac{\partial w}{\partial x}\right)]\, dV$$

Chapter 4 – Results and Discussion

4.1 Overview

In this section, the results of the free vibration for the parallelepiped rectangular beam are provided, as are the linear and nonlinear results involving the frequencies and mode shapes. Furthermore, the complete deformed shapes of the beam are given. The linear methodology his compared with the free vibration solutions depending on Euler–Bernoulli theory, and the nonlinear results are applied in terms of beam theory and the elasticity method, based on the nonlinearity of the Euler–Bernoulli theory and total Lagrange formulation, respectively.

4.2. Linear Analysis Results

The linear analysis considered a focused beam with the properties shown in Table 4.1. Ritz method approximation was used for the series functions, for various maximum powers, when $N = 6$, $N = 8$, and $N = 10$.

Table 4.1 Properties of the beam

Properties	Value
Modulus of elasticity, E	2.0
Length of the beam, L	10
Width of the beam, b	1.0
Poisson's ratio	0.0
Mass density	1.0
Thickness of beams, h	1.0

The first three natural frequencies of the Ritz method are shown in Tables 4.2, 4.3, and 4.4. The results were compared with the Euler–Bernoulli frequencies computed from Equation (3.13). As the length increased, the natural frequency becomes smaller.

Table 4.2 Natural frequency of the Ritz method for $N = 6$ of a Free–Free beam.

$N = 6$					
L = 5		*L = 10*		*L = 20*	
Ritz App.	*E.B. Theory*	*Ritz App.*	*E.B. Theory*	*Ritz App.*	*E.B. Theory*
0.3266	0.3654	0.0885	0.0913	0.0226	0.0228
0.7972	1.0071	0.2386	0.2518	0.0633	0.0629
1.3783	1.9743	0.4528	0.4936	0.1261	0.1234

Table 4.3 Natural frequency of the Ritz method for $N = 8$ of a Free–Free beam.

$N = 8$					
L = 5		*L = 10*		*L = 20*	
Ritz App.	*E.B. Theory*	*Ritz App.*	*E.B. Theory*	*Ritz App.*	*E.B. Theory*
0.3266	0.3654	0.0885	0.0913	0.0226	0.0228
0.7780	1.0071	0.2320	0.2518	0.0615	0.0629
1.3170	1.9743	0.4278	0.4936	0.1185	0.1234

Table 4.4 Natural frequency of the Ritz method for $N = 10$ of a Free–Free beam.

$N = 10$					
L = 5		*L = 10*		*L = 20*	
Ritz App.	*E.B. Theory*	*Ritz App.*	*E.B. Theory*	*Ritz App.*	*E.B. Theory*
0.3267	0.3654	0.0885	0.0913	0.0227	0.0228
0.7777	1.0071	0.2320	0.2518	0.0616	0.0629
1.3138	1.9743	0.4271	0.4936	0.1184	0.1234

The mode shapes for these assumptions are given in the following graphs, which were compared with the patterns of the Euler–Bernoulli mode shapes. The graphs show the coincidence of mode shapes between the Ritz approximations at various maximum powers and the Euler–Bernoulli Theory patterns, especially for the first two mode shapes.

The researcher has also noted that as the number of mode shapes increases, the accuracy of the low-power solutions decreases, as compared with the theoretical results. At the fourth mode, the shape pattern to the maximum power ($N = 10$) hardly forms mode shapes well as the Euler–Bernoulli theory's pattern does, as can be seen in Figure 4.2.

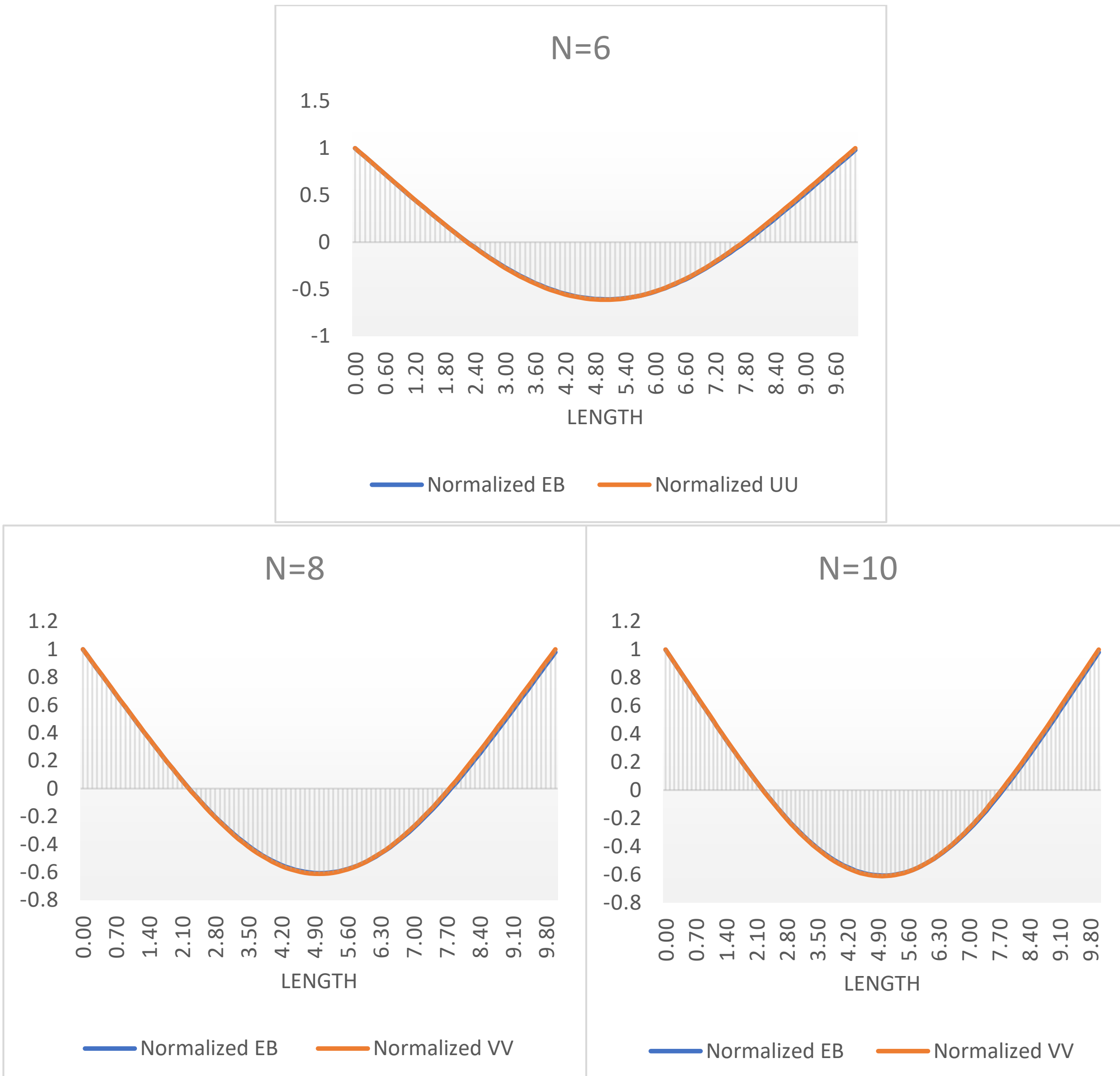

Figure 4.1 First mode shapes with $N = 6$, 8, and 10

In Figure 4.3, the oscillation values are connected with the length. The first four mode shapes are given in Appendix A. This assumption was tested with lengths of 10 and 5.

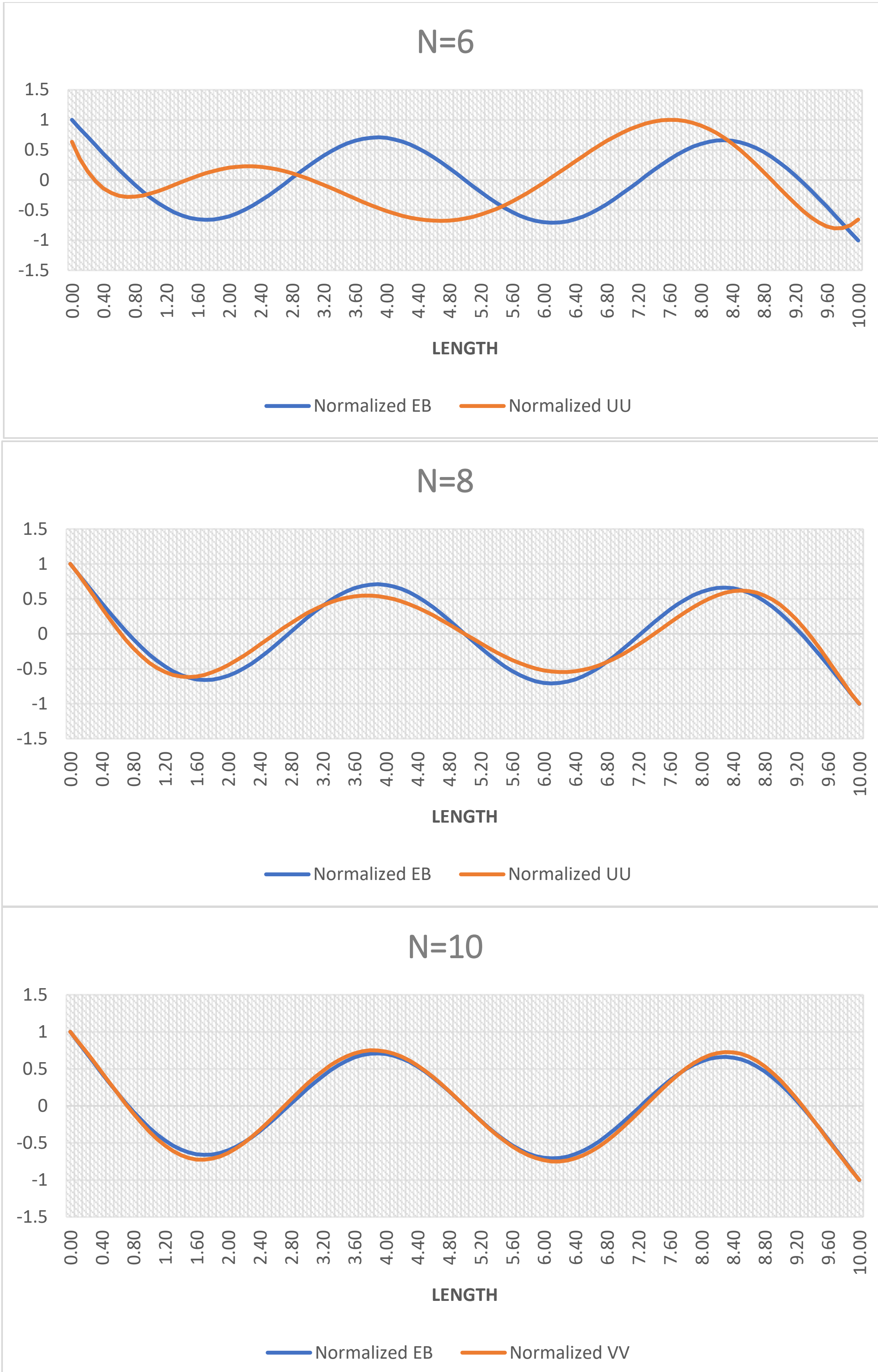

Figure 4.2 Accuracy of various N values for the fourth mode's shapes

The results show that as the beam's thickness increases, the frequencies tend to be more elastic, as shown in Figure 4.3, in comparison with the exact oscillations.

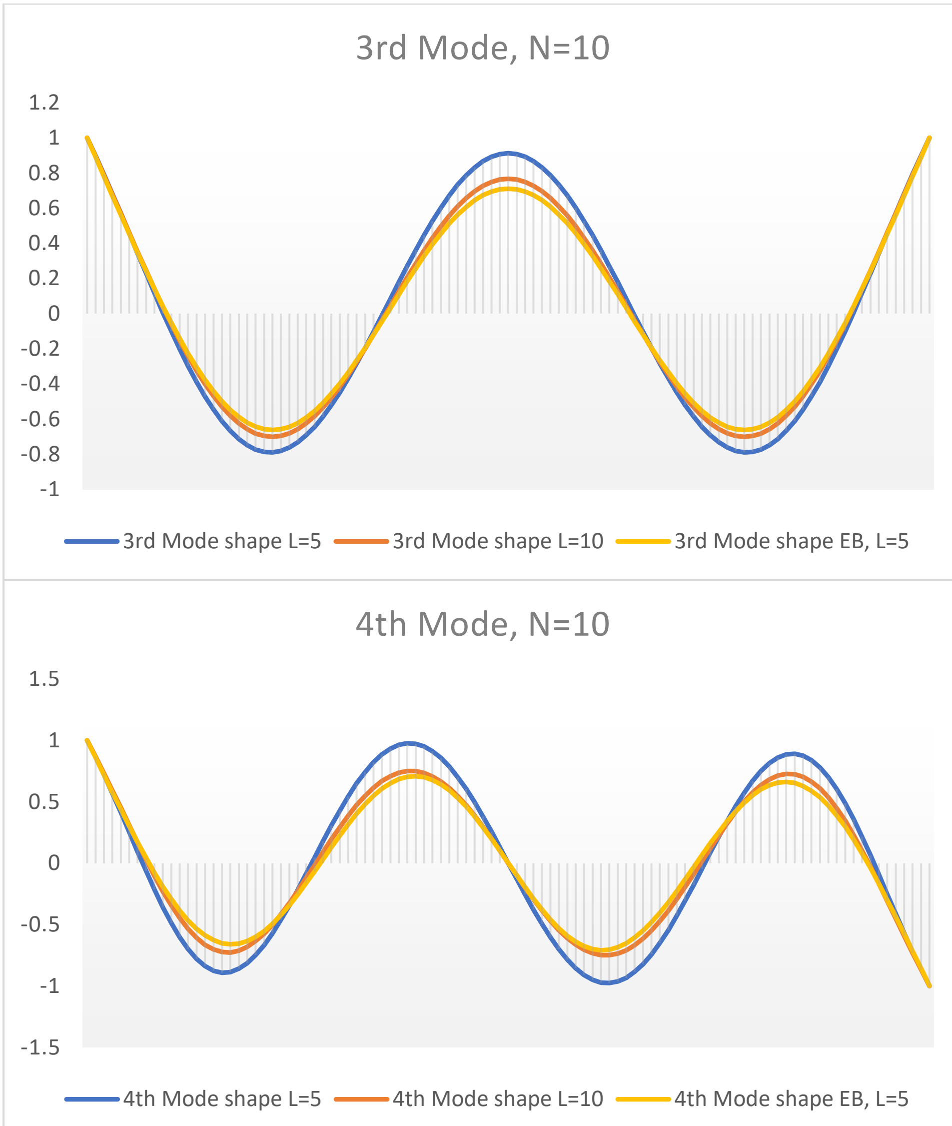

Figure 4.3 Frequencies of various lengths for the third and fourth mode shapes

In addition, the impact of the maximum power (N) in the frequencies was compared to that of the exact solution. As N increases, the frequencies tend to become more uniformly distributed. This supports the accuracy of the mode shapes with the increments of N mentioned above in this chapter.

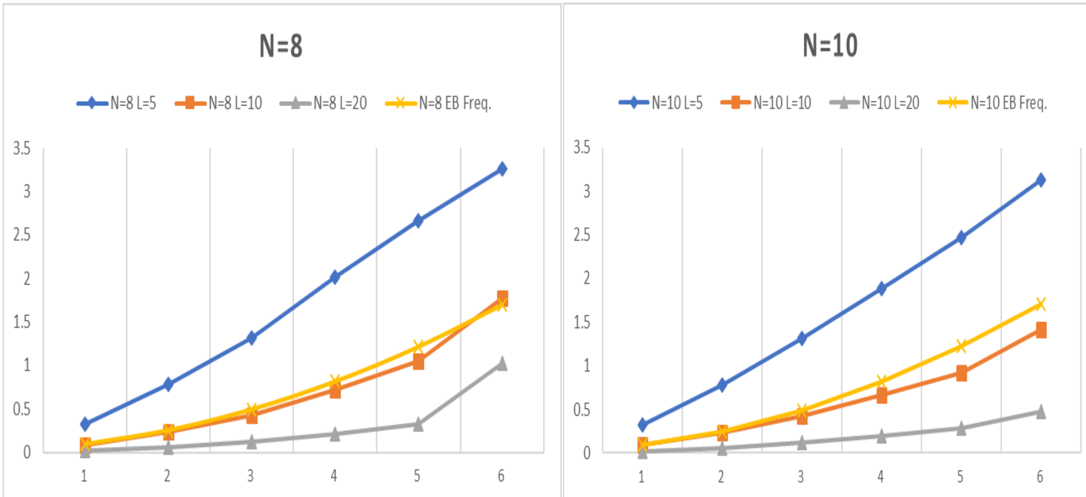

Figure 4.4 Frequency values of various maximum powers (*N*)

Figures 4.5, 4.6, and 4.7 show the three-dimensional deformed shapes computed with the elasticity method. The beam was meshed with hexahedral elements, and the displacements *u*, *v*, and *w* were applied to each node, as can be seen in the following deformed shapes. The largest displacements in a specific direction led the beam to deformed about that direction axis for *x*, *y*, or *z*.

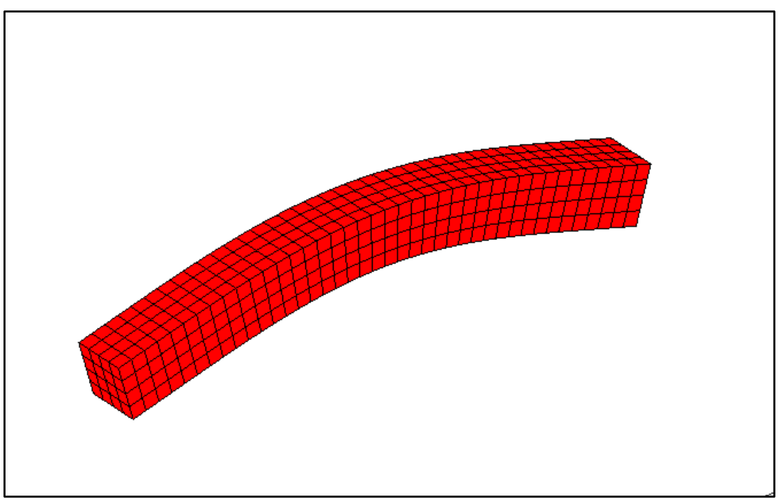
Figure 4.5 Deformed shape of the first mode of a three-dimensional free–free beam

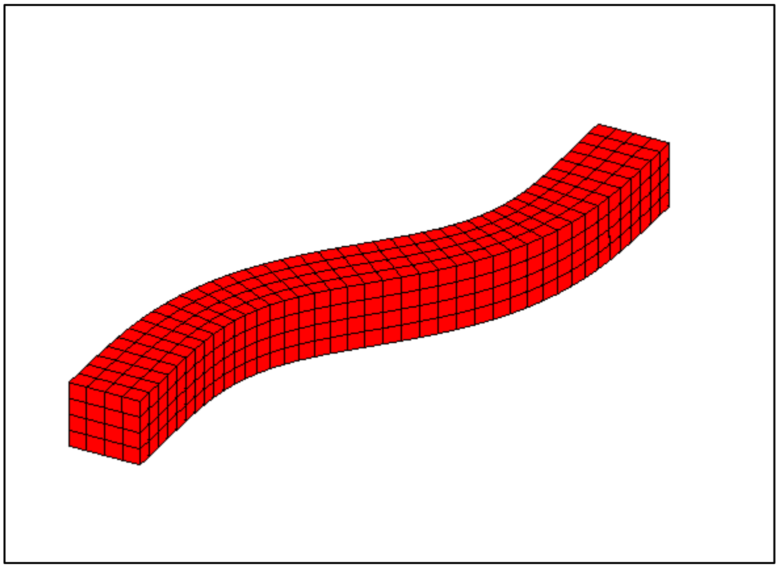

Figure 4.6 Deformed shape of the second mode of a three-dimensional free–free beam

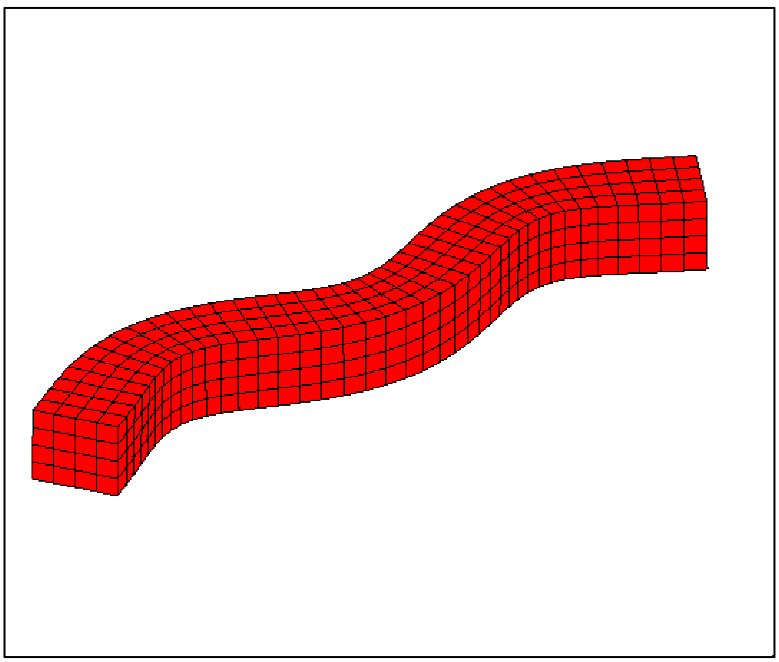

Figure 4.7 Deformed shape of the third mode of a three-dimensional free–free beam

4.3 Nonlinear Analysis Results

4.3.1 Nonlinear Beam Theory

The nonlinear analysis was based on Lagrange and Hermite interpolations. In nonlinear vibration, increases in oscillation are caused by the contribution of the axial force to the bending frequency due to the beam stretching. Various boundary conditions were examined for the nonlinear vibrations. All of the results showed good agreement with two publications introduced in the literature review (Evensen, 1968; Woinowsky-Krieger, 1950). Tables 4.5, 4.6, and 4.7 give the frequency ratio $(\omega_{NL}/\omega_L)^2$ of various boundary conditions for 4, 8, and 16 elements.

Table 4.5 $(\omega_{NL}/\omega_L)^2$ of a simply–simply supported beam

a/r	One–dimensional Nonlinear EB model			Woinowsky-Krieger (1950)
	$n = 4$	$n = 8$	$n = 16$	
0.1	1.0027	1.0026	1.0025	1.0025
0.2	1.0109	1.0102	1.0100	1.0100
0.4	1.0434	1.0408	1.0400	1.0400
0.6	1.0977	1.0917	1.0900	1.0900
0.8	1.1736	1.1631	1.1601	1.1600
1	1.2712	1.2548	1.2501	1.2500
1.5	1.6099	1.5730	1.5626	1.5625
2	2.0834	2.0182	1.9998	2.0000
2.5	2.6912	2.5901	2.5611	2.5625
3	3.4326	3.2881	3.2464	3.2500
3.5	4.3068	4.1120	4.0551	4.0625
4	5.3131	5.0609	4.9866	5.0000

Table 4.6 $(\omega_{NL}/\omega_L)^2$ of a clamped–clamped beam

a/r	One–dimensional Nonlinear EB model			Continuum Solutions	
	$n = 4$	$n = 8$	$n = 16$	Krieger (1950)	Evensen (1968)
0.1	1.0009	1.0007	1.0006	1.0006	1.0006
0.2	1.0034	1.0026	1.0024	1.0024	1.0024
0.4	1.0137	1.0104	1.0098	1.0096	1.0096
0.6	1.0307	1.0234	1.0220	1.0216	1.0216
0.8	1.0546	1.0416	1.0390	1.0383	1.0384
1	1.0852	1.0650	1.0609	1.0598	1.0599
1.5	1.1910	1.1459	1.1368	1.1343	1.1349
2	1.3379	1.2587	1.2425	1.2382	1.2398
2.5	1.5246	1.4029	1.3775	1.3708	1.3750
3	1.7496	1.5777	1.5412	1.532	1.5396
3.5	2.0114	1.7824	1.7328	1.7211	1.7350

The oscillations were taken with consideration of the a/r ratio, for which a is the peak amplitude and r is the radius of gyrations, aimed at nondimensionalizing the amplitude values. The results were also compared with those of Evensen (1968).

Table 4.7 $(\omega_{NL}/\omega_L)^2$ of a clamped–simply supported beam

a/r	One–dimensional Nonlinear EB model			Continuum Solutions	
	$n = 4$	$n = 8$	$n = 16$	Krieger (1950)	Evensen (1968)
0.1	1.0015	1.0014	1.0013	1.0013	1.0013
0.2	1.0063	1.0056	1.0053	1.0053	1.0053
0.4	1.0252	1.0222	1.0214	1.0213	1.0214
0.6	1.0566	1.0499	1.0481	1.0479	1.0481
0.8	1.1004	1.0887	1.0856	1.0850	1.0854
1	1.1567	1.1385	1.1336	1.1323	1.1335
1.5	1.3509	1.3103	1.2994	1.2947	1.3004
2	1.6196	1.5486	1.5295	1.5175	1.5340
2.5	1.9602	1.8509	1.8215	1.7978	1.8344
3	2.3695	2.2143	2.1727	2.1331	2.2015
3.5	2.8441	2.6350	2.5791	2.5217	2.6354

4.3.2 Nonlinear Elasticity Analysis

The two-dimensional clamped–clamped beam was investigated by using the elasticity method. The investigation was done using the methodology described in Section 3.3.2, and the outcomes were compared with the results of continuum solutions and higher-order theory (Evensen, 1968; Heyliger & Reddy, 1988a; Woinowsky-Krieger, 1950).

The investigation was applied for the approximation functions when $N = 4$ and $N = 6$, where N is the maximum number of the approximation functions. The displacement components u and w (in the two-dimensional case) were targeted in the research, based on Euler–Bernoulli theory. The vibrational behavior at $N = 4$ is given in Table 4.8. The frequencies were smaller than the Euler-Bernoulli frequencies when $L = 10$ and 20, respectively.

When $L = 4$, the oscillations become larger than the exact solution, as the elastic condition was compared with the fixed exact formulations.

Table 4.8 Nonlinear frequency of a clamped–clamped beam of $N = 4$

a/r	*L = 4*		*L = 10*		*L = 20*	
	Ritz App.	*Non. E.B.*	*Ritz App.*	*Non. E.B.*	*Ritz App.*	*Non. E.B.*
0.4	1.0127	1.0097	1.0093	1.0098	1.0081	1.0098
1	1.0790	1.0605	1.0577	1.0650	1.0505	1.0610
1.5	1.1767	1.1358	1.1294	1.1459	1.1133	1.1369
2	1.3116	1.2405	1.2290	1.2587	1.2006	1.2428
2.5	1.4818	1.3741	1.3558	1.4029	1.3117	1.3780
3	1.6848	1.5357	1.5088	1.5777	1.4459	1.5420
3.5	1.9174	1.7241	1.6867	1.7824	1.6020	1.7340

When $N = 6$, the frequencies were in good agreement with the results of higher-order theory, when the Hermite and Lagrange interpolations of the finite elements' formulation were applied. As can be seen in Table 4.9, the nonlinear frequencies tend to be larger as the length decreases.

Table 4.9 Nonlinear frequency of a clamped–clamped beam of $N = 6$

a/r	*L* = 4	*L* = 10	*L* = 20	*L* = 40	Heyliger and Reddy
0.4	1.0128	1.0104	1.0101	1.0100	1.01065
1	1.0799	1.0645	1.0627	1.0622	1.06679
1.5	1.1787	1.1445	1.1405	1.1395	1.14956
2	1.3148	1.2553	1.2483	1.2466	1.26428
2.5	1.4858	1.3956	1.3852	1.3827	1.41003
3	1.6883	1.5639	1.5498	1.5465	1.58596
3.5	1.9178	1.7582	1.7405	1.7365	1.79129
4	2.1676	1.9763	1.9556	1.9510	2.02538

Various a/r ratios were also inspected along the given lengths of this model. On the other hand, the Gaussian points and weights' impacts were examined for $N = 6$ with $L = 10$ and 20. The objective of this parameter was to study the accuracy of the elasticity results as the Gaussian point numbers increase. Table 4.10 shows the effect of the increased Gaussian points and weights on the nonlinear frequencies and the ratio between them.

Table 4.10 Accuracy of the frequencies based on Gaussian points and weights

Gaussian Points and Weights	$a/r = 1$		$a/r = 2$	
	$L = 10$	$L = 20$	$L = 10$	$L = 20$
24 points	1.0609	1.0571	1.2419	1.2270
8 points	1.0645	1.0627	1.2553	1.2483
Ratio %	0.3436	0.5260	1.0705	1.7035
Heyliger and Reddy	1.06679		1.26428	

The impact of increasing the Poisson's ratio on the natural frequency was studied for this research. The results show that the frequencies increase when $\upsilon = 0.3$ is in compression with $\upsilon = 0$. However, the $(\omega_{NL}/\omega_L)^2$ was slightly affected based on the Poisson's ratio. Tables 4.11 and 4.12 give the first linear and nonlinear frequencies, with the consideration of various Poisson's ratios.

The results were compared by length (4, 10, 20, and 40) by the maximum number of used functions (N). The complete linear and nonlinear results are shown in Appendix A with a/r ratios of 0.4, 1.0, and 2.0.

Table 4.11 Linear frequency of $\upsilon = 0$ and $\upsilon = 0.3$ for a C–C beam

$a/r = 1.0$				$a/r = 1.0$			
$N = 6$				$N = 4$			
$L = 10$		$L = 4$		$L = 10$		$L = 4$	
$\upsilon = 0$	$\upsilon = 0.3$	$\upsilon = 0$	$\upsilon = 0.3$	$\upsilon = 0$	$\upsilon = 0.3$	$\upsilon = 0$	$\upsilon = 0.3$
0.00763	0.01099	0.19907	0.25711	0.00853	0.01198	0.20333	0.26372
0.05378	0.07541	1.02448	1.19746	0.05965	0.08476	1.1109	1.35293
0.1381	0.16771	1.22869	1.42461	0.19739	0.27447	1.2337	1.82347
0.1431	0.18132	1.32955	1.81053	0.2055	0.29124	3.03278	3.52172

Table 4.12 Nonlinear frequency of $\upsilon = 0$ and $\upsilon = 0.3$ for a C–C beam

$a/r = 1.0$				$a/r = 1.0$			
$N = 6$				$N = 4$			
$L = 10$		$L = 4$		$L = 10$		$L = 4$	
$\upsilon = 0$	$\upsilon = 0.3$	$\upsilon = 0$	$\upsilon = 0.3$	$\upsilon = 0$	$\upsilon = 0.3$	$\upsilon = 0$	$\upsilon = 0.3$
0.00812	0.01175	0.21499	0.279259	0.00902	0.01278	0.21938	0.28724
0.05362	0.07434	0.97236	1.127736	0.0595	0.08387	1.03338	1.25177
0.13772	0.16688	1.27453	1.361043	0.19773	0.27404	1.31848	1.90904
0.14294	0.1792	1.33012	1.891309	0.20546	0.29156	2.96741	3.44127

The ratios of nonlinear frequency to the linear frequency was computed. The values were compared with the ratios of $\upsilon = 0$. Tables 4.13 and 4.14 show that the ratios slightly increased when the Poisson's ratio increased.

Table 4.13 Comparison of $(\omega_{NL}/\omega_L)^2$ for $N = 4$

N = 4		*L = 4*	*L = 10*	*L = 20*	*L = 40*
a/r = 0.4	υ = 0	1.0127	1.0093	1.0081	1.0080
	υ = 0.3	1.0144	1.0107	1.0099	1.0096
a/r = 1.0	υ = 0	1.0790	1.0577	1.0505	1.0496
	υ = 0.3	1.0892	1.0669	1.0615	1.0598
a/r = 1.5	υ = 0	1.1767	1.1294	1.1133	1.1114
	υ = 0.3	1.1984	1.0615	1.1377	1.0615
a/r = 2.0	υ = 0	1.3116	1.2290	1.2006	1.1975
	υ = 0.3	1.3467	1.2638	1.2434	1.2375
a/r = 2.5	υ = 0	1.4818	1.3558	1.3117	1.3072
	υ = 0.3	1.5294	1.4079	1.3772	1.5294
a/r = 3	υ = 0	1.6848	1.5088	1.4459	1.4401
	υ = 0.3	1.7393	1.5797	1.5378	1.5276
a/r = 3.5	υ = 0	1.9174	1.6867	1.6020	1.5954
	υ = 0.3	1.9671	1.7767	1.7233	1.7121
a/r = 4.0	υ = 0	2.1755	1.8883	1.7791	1.7723
	υ = 0.3	2.1999	1.9957	1.9316	1.9211

Table 4.14 Comparison of $(\omega_{NL}/\omega_L)^2$ for $N = 6$

N = 6		*L = 4*	*L = 10*	*L = 20*	*L = 40*
a/r = 0.4	υ = 0	1.0128	1.0104	1.0101	1.0100
	υ = 0.3	1.0139	1.0112	1.0109	1.0109
a/r = 1.0	υ = 0	1.0799	1.0645	1.0627	1.0622
	υ = 0.3	1.0861	1.0693	1.0681	1.0679
a/r = 1.5	υ = 0	1.1787	1.1445	1.1405	1.1395
	υ = 0.3	1.1903	1.1545	1.1520	1.1516
a/r = 2.0	υ = 0	1.3148	1.2553	1.2483	1.2466
	υ = 0.3	1.3286	1.2709	1.2672	1.2667
a/r = 2.5	υ = 0	1.4858	1.3956	1.3852	1.3827
	υ = 0.3	1.4914	1.4151	1.4109	1.4106
a/r = 3	υ = 0	1.6883	1.5639	1.5498	1.5465
	υ = 0.3	1.6619	1.5815	1.5786	1.5790
a/r = 3.5	υ = 0	1.9178	1.7582	1.7405	1.7365
	υ = 0.3	1.8108	1.7612	1.7634	1.7654
a/r = 4.0	υ = 0	2.1676	1.9763	1.9556	1.9510
	υ = 0.3	1.7591	1.9381	1.9526	1.9581

Chapter 5 – Conclusion

A three-dimensional rectangular parallelepiped beam was examined for linear vibration analysis using the Ritz approximation method. The Euler–Bernoulli beam theory was also applied to validate this approximation. For the nonlinear analysis, a two-dimensional clamped–clamped beam was investigated based on the total Lagrange formulation. The nonlinear Euler–Bernoulli theory was used to compare the outcomes of the elasticity methods.

5.1 Concluding Remarks

In the linear vibration analysis, the Ritz method was applied for the free–free three-dimensional beam in terms of power series functions of the Cartesian coordinate system. The maximum power numbers analyzed were 6, 8, and 10, along with the related degrees of freedom. The natural frequency of this approximation was computed based on these power series. As part of the evaluation of the followed formulation, the natural frequency was solved depending on the Euler–Bernoulli theory, which had good agreement with lengths of the modeled beam of 5, 10, and 20. In addition, the mode shapes were computed with Ritz approximation. All of the patterns were compared with Euler–Bernoulli mode shapes. The results show that as maximum power increased, the mode shapes tended to become closer to the Euler–Bernoulli patterns. However, the various lengths showed the elastic status of the approximated method, especially when $L = 5$. Generally, the outcomes of the free–free beam approximation validated the Ritz method in comparison with the beam theory results.

For the nonlinear study, a two-dimensional clamped–clamped beam was investigated. The approximation method was formulated based on the total Lagrange formulation. This formulation took into consideration the impacts of second Piola–Kirchhoff stresses and Green–Lagrange strain. The Euler–Bernoulli beam theory was applied for a one-dimensional rectangular beam based on Hermite and Lagrange interpolations with various boundary conditions. The frequencies were found according to elements of 4, 8, and 16. The ratios for natural frequency based on beam theory were in good agreement with Woinowsky-Krieger (1950) and Evensen (1968). The solution for the nonlinear equations was applied by using the direct iteration method, as described in Chapter 3. However, the natural frequency ratios of the elasticity method agreed with those of higher order theory from Heyliger and Reddy (1988a).

The effects of the number of Gaussian points and weights were examined by considering 8 and 24 points. The frequency tends to be more accurate as the applied Gaussian points increase, but this does not eliminate the results of the lower Gaussian evaluation. Depending on the results, the difference in the frequency of the studied Gauss numbers ranges from 0.3% to 1.8%, which is acceptable. The frequencies were computed for both beam theory and the elasticity method, for various lengths of the modeled two- and one-dimensional beams, respectively. The Poisson's ratio was assumed to be 0 or 0.3 for the isotropic material. The ratio of nonlinear to linear frequency showed a slight increase as Poisson's ratio increased. The natural frequencies for the various boundary conditions of the beam theory are provided in Appendix A, along with the natural frequency of elasticity.

5.2 Future Work

For the linear model, a work should study the impact of a maximum power larger than 10 for the Ritz approximation on the natural frequency and mode shapes. In addition, future work should impose various boundary conditions instead of the free–free beam model. Investigations should also include various kinds of applied functions and their outcomes in the Cartesian power series. Regarding the nonlinear analysis, the Poisson's ratio should be increased to 0.5, and other boundary conditions should be imposed. The two-dimensional model should also be extended to the three-dimensional model, with consideration of the various martial properties and geometries, to examine their effects on dynamic behavior.

References

Apiwattanalunggarn, P., Shaw, S. W., Pierre, C., & Jiang, D. (2003). Finite-element-based nonlinear modal reduction of a rotating beam with large-amplitude motion. *Modal Analysis*, *9*(3–4), 235–263.

Aydogdu, M. 2006. Buckling analysis of cross-ply laminated beams with general boundary conditions by Ritz method. *Composites Science and Technology*, *66*(10), 1248–1255.

Bathe, K.-J., Ramm, E., & Wilson, E. L. (1975). Finite element formulations for large deformation dynamic analysis. *International Journal for Numerical Methods in Engineering*, *9*, 353–386.

Bhashyam, G. R., & Prathap, G. (1980). *Galerkin finite element method for non-linear beam vibrations*. *Name of Journal*, *72*(2), 191–203.

Chatterjee, A. (2009, February). A brief introduction to nonlinear vibrations. *IITK*. Retrieved from http://home.iitk.ac.in/~anindya/NLVnotes.pdf

Chen, D., Kitipornchai, S., & Yang, J. (2016). Nonlinear free vibration of shear deformable sandwich beam with a functionally graded porous core. *Thin-Walled Structures*, *107*, 39–48.

Dupuis, G. A., Hibbitt, H. D., McNamara, S. F., & Marcal, P. V. (1971). Nonlinear material and geometric behavior of shell structures. *Computers and Structures*, *1*(1–2), 223–239.

Eer Nisse, E. P. (1967). Variational method for electroelastic vibration analysis. *IEEE Transactions on Sonics and Ultrasonics*, *14*(4), 153–160.

Evensen, D. A. (1968). Nonlinear vibrations of beams with various boundary conditions. *AIAA Journal*, *6*(2), 370–372.

Ghasemi, A. R., Taheri-Behrooz, F., Farahani, S. M. N., & Mohandes, M. (2016). Nonlinear free vibration of an Euler-Bernoulli composite beam undergoing finite strain subjected to different boundary conditions. *Journal of Vibration and Control*, *22*(3), 799–811.

Hamdan, M. N., & Shabaneh, N. H. (1997). Large amplitude free vibrations of a uniform cantilever beam carrying an intermediate lumped mass and rotary inertia. *Journal of Sound and Vibration*, *206*(issue), 151–168.

Heyliger, P. R., & Jilani, A. (1992). The free vibrations of inhomogeneous elastic cylinders and spheres. *International Journal of Solids and Structures*, *29*(22), 2689–2708.

Heyliger, P. R., & Reddy, J. N. (1988a). A higher order beam finite element for bending and vibration problems. *Journal of Sound and Vibration*, 126(2), 309–326.

Heyliger, P. R., & Reddy, J. N. (1988b). On a mixed finite element model for large deformation analysis of elastic solids. *International Journal of Non-Linear Mechanics*, *23*(2), 131–145.

Hibbitt, H. D., Marcal, P. V., & Rice, J. R. (1970). A finite element formulation for problems of large strain and large displacement. *International Journal of Solids and Structures*, *volume*(1-2), 223–239.

Ke, L. L., Wang, Y. S., Yang, J., & Kitipornchai, S. (2012). Nonlinear free vibration of size-dependent functionally graded microbeams. *International Journal of Engineering Science*, *50*(2012), 256–267.

Ke, L. L., Yang, J., & Kitipornchai, S. (2010). Nonlinear free vibration of functionally graded carbon nanotube-reinforced composite beams. *Composite Structures*, *92*(3), 676–683.

Kiani Y., & Mirzaei, M. (2016). Thermal postbuckling of temperature-dependent sandwich beams with carbon nanotube-reinforced face sheets. *Journal of Thermal Stresses*, *39*(9), 1098–1110.

Kitipornchai, S., Ke, L. L., Yang, J., & Xiang, Y. (2009). Nonlinear vibration of edge cracked functionally graded Timoshenko beams. *Journal of Sound and Vibration*, *324*(3–5), 962–982.

Lewandowski, R. (1987). Application of the Ritz method to the analysis of non-linear free vibrations of beams. *Journal of Sound and Vibration*, *114*(1), 91–101.

Ma, H. M., Gao, X. L., & Reddy, J. N.. (2008). A microstructure-dependent Timoshenko beam model based on a modified couple stress theory. *Journal of the Mechanics and Physics of Solids*, *56*(12), 3379–3391.

Marur, S. R., & Prathap, G. (2005). Non-linear beam vibration problems and simplifications in finite element models. *Computational Mechanics*, *35*(5), 352–360.

Mei, C. (1973). Finite element displacement method for large amplitude free flexural vibrations of beams and plates. *Computers and Structures*, *3*, 163–174.

Ohno, I. (1976). Free vibration of a rectangular parallelepiped crystal and its application to determination of elastic constants of orthorhombic crystals. *Journal of Physics of the Earth*, *24*(4), 355–379.

Rao, S. S. (2007). *Vibration of continuous systems*. Hoboken, NJ: John Wiley & Sons.

Reddy, J. N. (2006). *An introduction to the finite element method*. Hightstown, NJ: McGraw-Hill.

Reddy, J. N. (2007). Nonlocal theories for bending, buckling and vibration of beams. *International Journal of Engineering Science*, *45*(2–8), 288–307.

Shen, H.-S. (2011). A novel technique for nonlinear analysis of beams on two-parameter elastic foundations. *International Journal of Structural Stability and Dynamics*, *11*(6), 999–1014.

Shen, H.-S., & Xiang, Y. (2013). Nonlinear analysis of nanotube-reinforced composite beams resting on elastic foundations in thermal environments. *Engineering Structures*, *56 (2013)*, 698–708.

Szemplinska-Stupnicka, W. (1983). “Non-linear normal modes” and the generalized Ritz method in the problems of vibrations of non-linear elastic continuous systems. *International Journal of Non-Linear Mechanics*, *18*(2), 149–165.

Venkateswara Rao, G., Kanaka Raju, K., & Raju, I. S. (1976). Finite element formulation for the large amplitude free vibrations of beams and orthotropic circular plates. *Computers and Structures*, *6*(issue), 169–172.

Visscher, William M., Migliori, Albert., Bell, Thomas M., & Reinert, Robert A. (2008). On the normal modes of free vibration of inhomogeneous and anisotropic elastic objects. *The Journal of the Acoustical Society of America*, *90*(4), 2154-2162.

Wilson, E. L., Farhoomand, I., & K. J. Bathe. (1973). Nonlinear dynamic analysis of complex structures. *Earthquake Engineering and Structural Dynamics*, *1*, 241–252.

Woinowsky-Krieger, S. (1950). The effect of an axial force on the vibration of hinged bars. *Journal of Applied Mechanics*.

Appendix A

In the first section of this appendix, the mode shapes from the linear-vibration analysis are compared with those from the beam-theory results. In the second section, the mode shapes from nonlinear Euler–Bernoulli theory are presented. In the last section, the linear and nonlinear frequencies of the iteration method, as well as the nonlinear frequencies from Euler–Bernoulli theory, are shown.

A.1 Linear Analysis Results

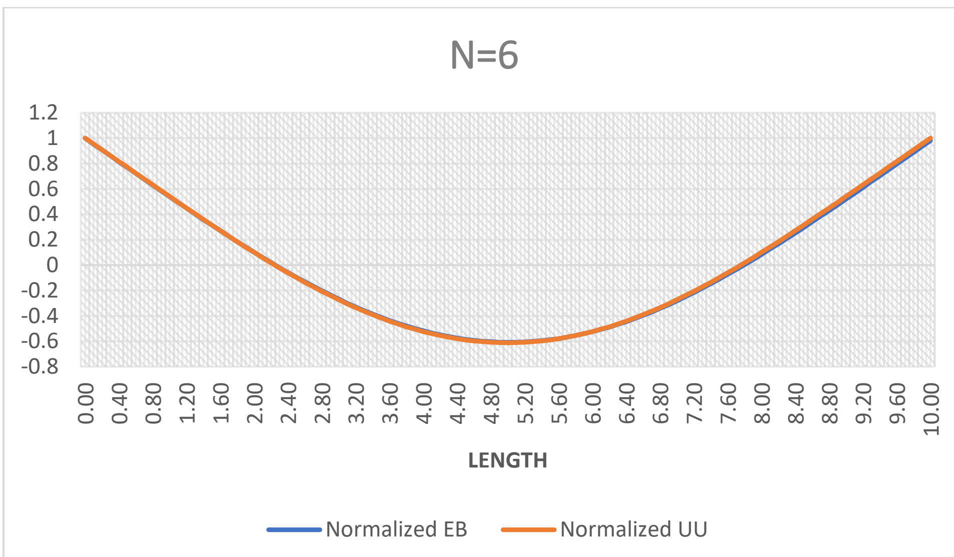

Figure A.1.1 First mode shape in comparison with the Euler–Bernoulli mode shape for $N = 6$

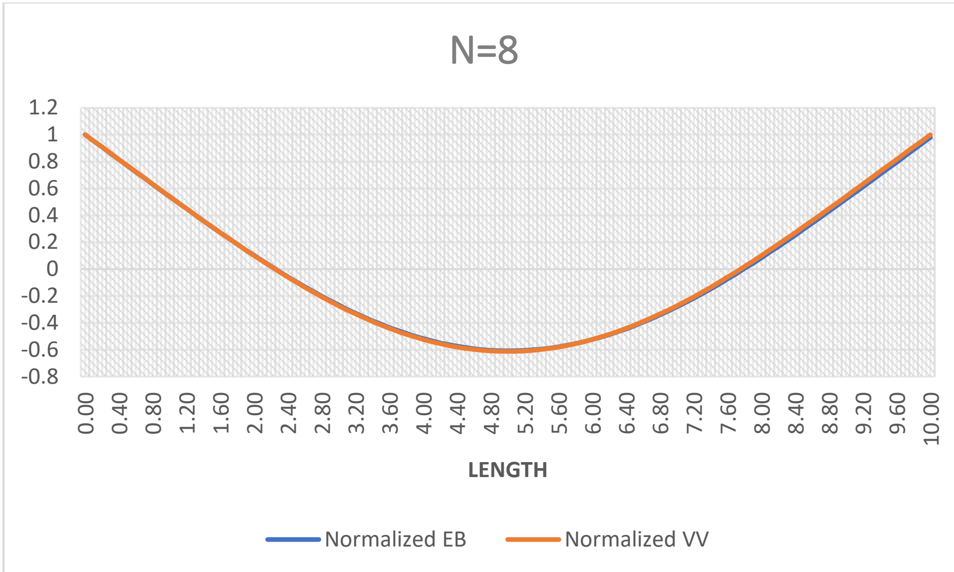

Figure A.1.2 First mode shape compared with the Euler–Bernoulli mode shape for $N = 8$

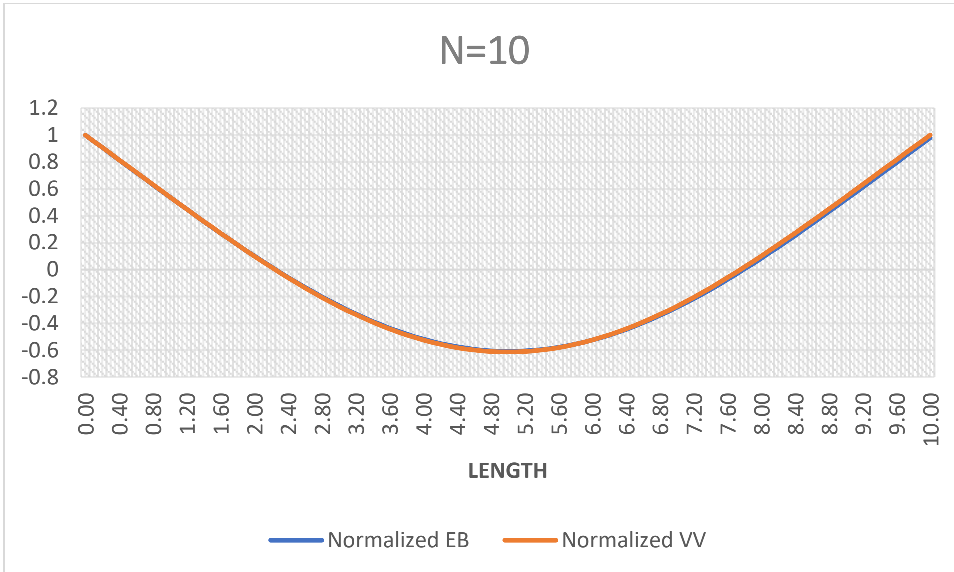

Figure A.1.3 First mode shape compared with the Euler–Bernoulli mode shape for $N = 10$

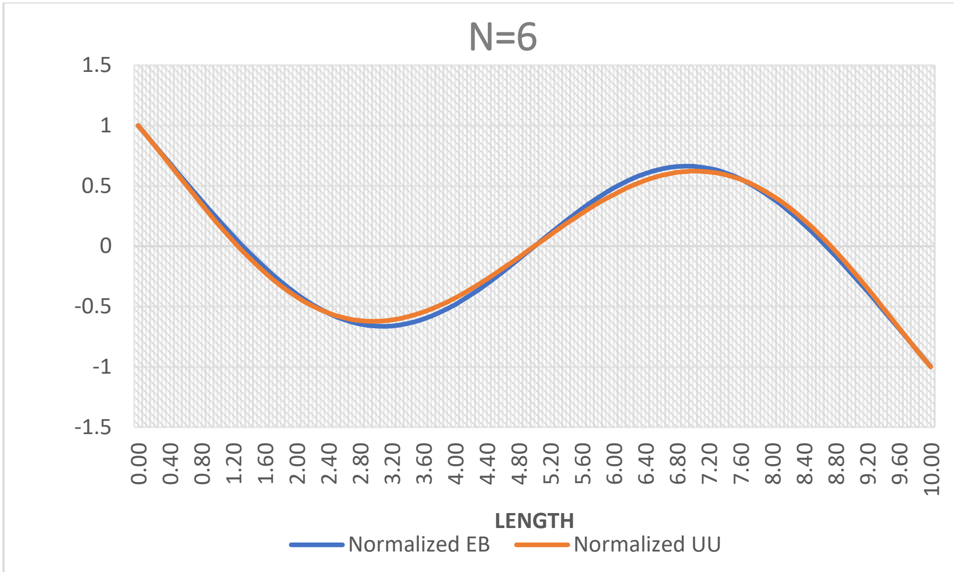

Figure A.1.4 Second mode shape compared with the Euler–Bernoulli mode shape for $N = 6$

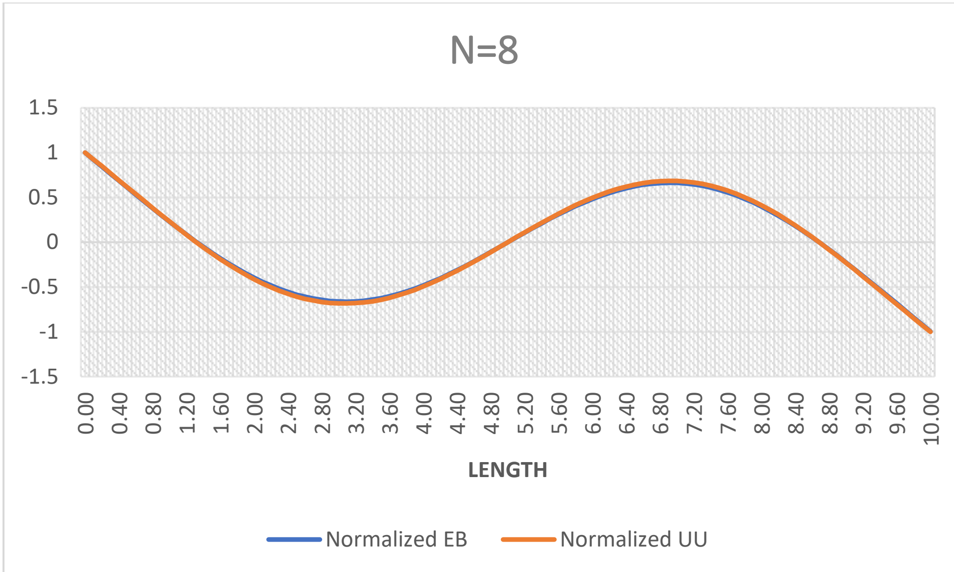

Figure A.1.5 Second mode shape compared with the Euler–Bernoulli mode shape for $N = 8$

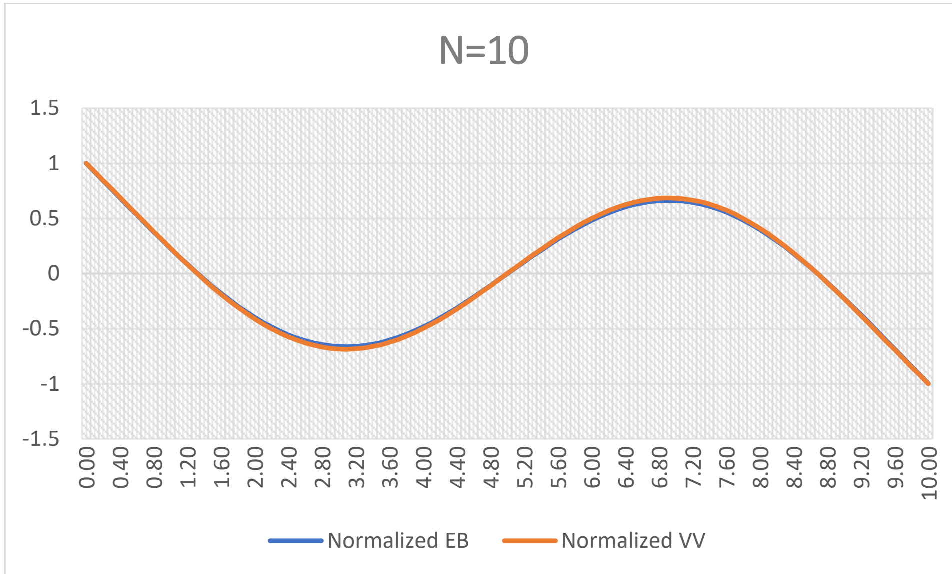

Figure A.1.6 Second mode shape compared with the Euler–Bernoulli mode shape for $N = 10$

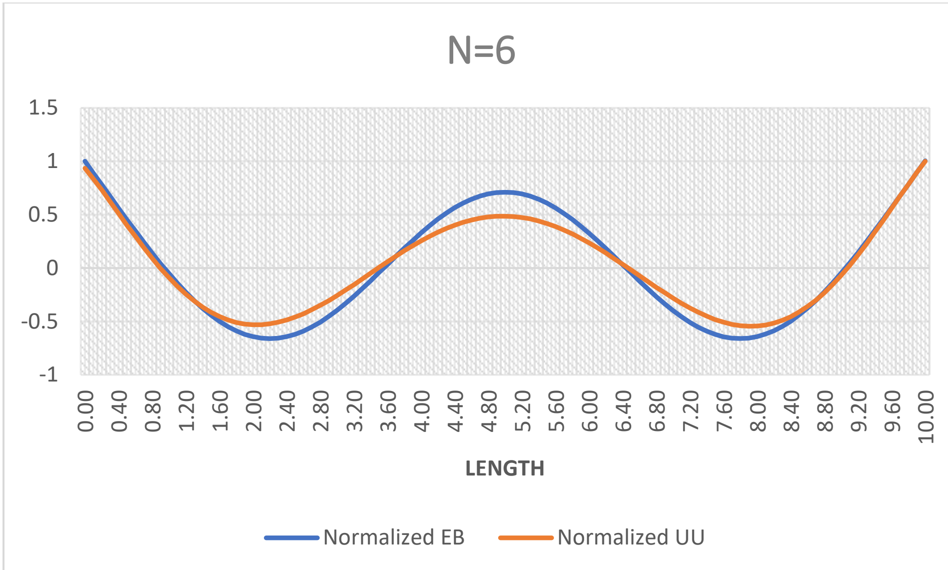

Figure A.1.7 Third mode shape compared with the Euler–Bernoulli mode shape for $N = 6$

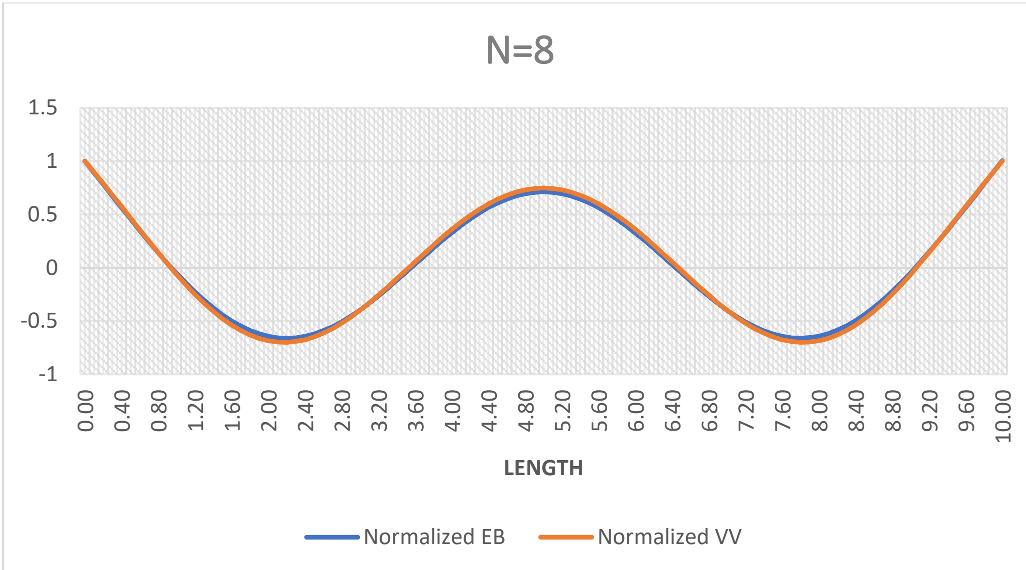

Figure A.1.8 Third mode shape compared with the Euler–Bernoulli mode shape for $N = 8$

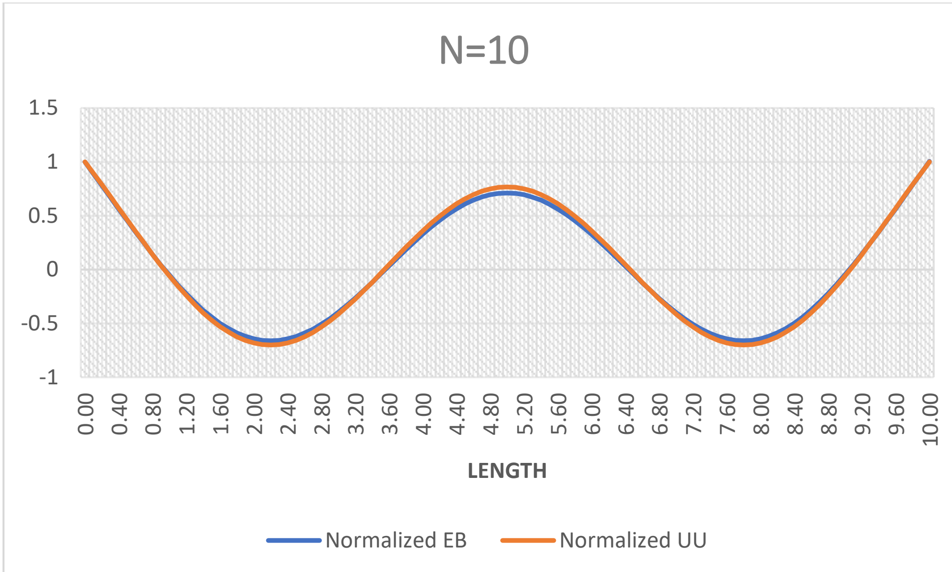

Figure A.1.9 Third mode shape compared with the Euler–Bernoulli mode shape for $N = 10$

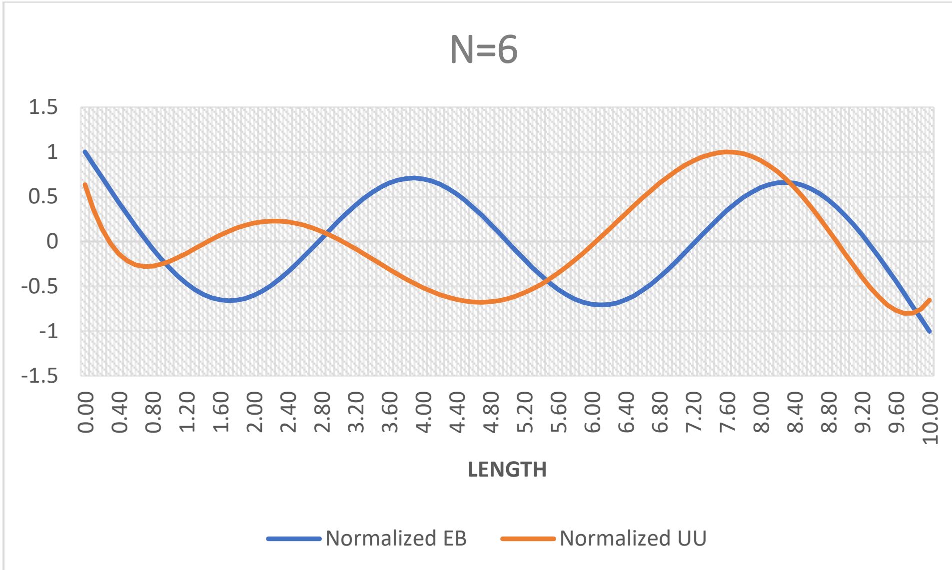

Figure A.1.10 Fourth mode shape compared with the Euler–Bernoulli mode shape for $N = 6$

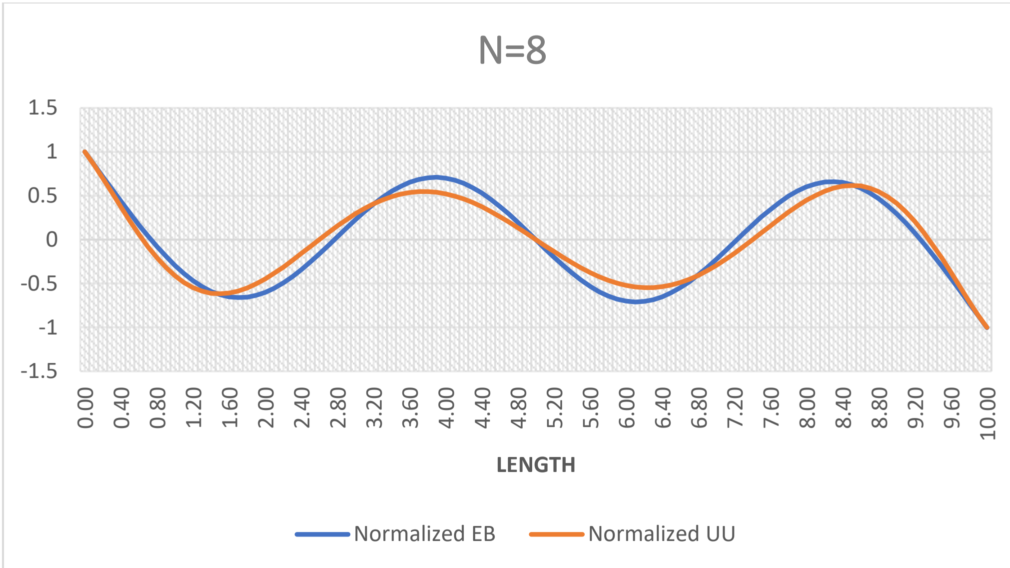

Figure A.1.11 Fourth mode shape compared with the Euler–Bernoulli mode shape for $N = 8$

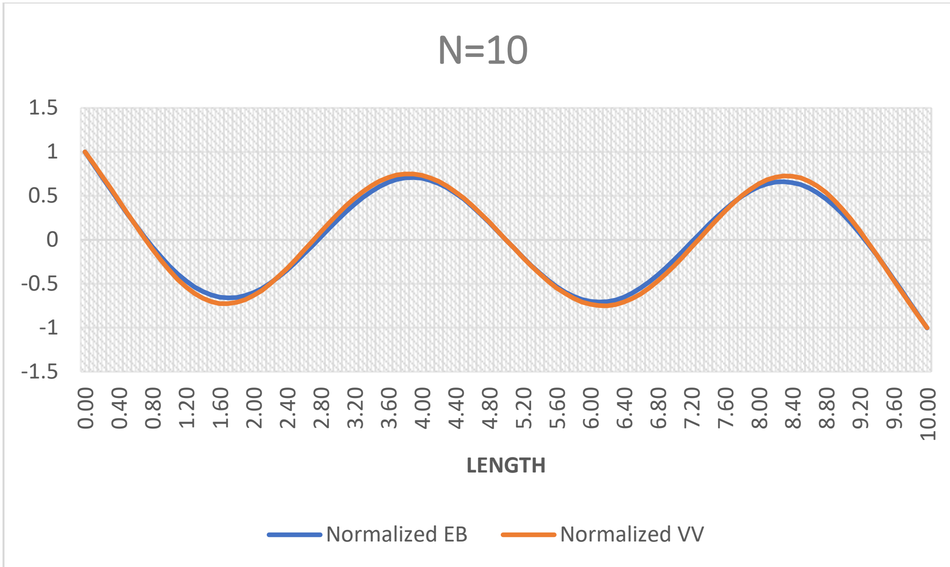

Figure A.1.12 Fourth mode shape compared with the Euler–Bernoulli mode shape for $N = 10$

A.2 The Effect of the Various Lengths on the Linear Mode Shapes

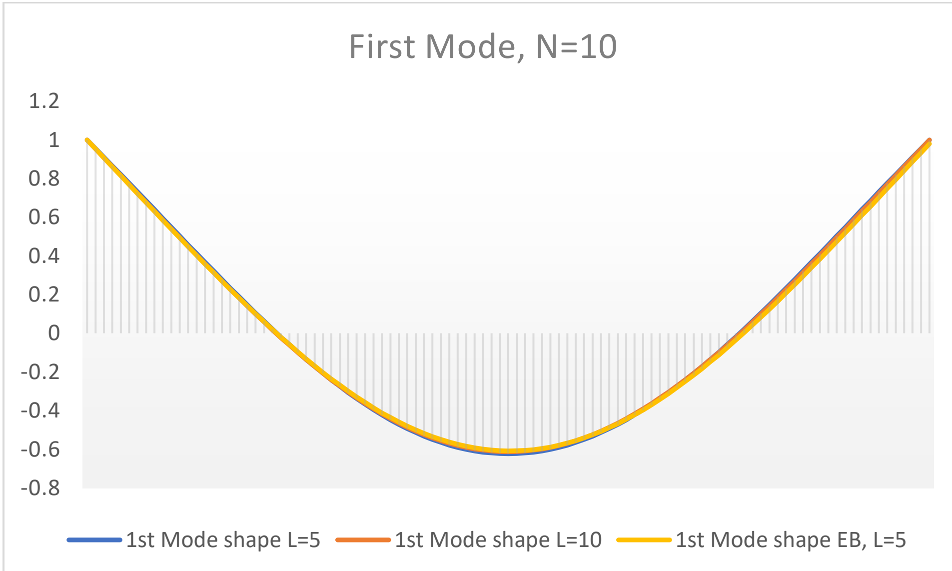

Figure A.2.1 First mode shape for $L = 10$ and 5 compared with the Euler–Bernoulli mode shape for $N = 10$

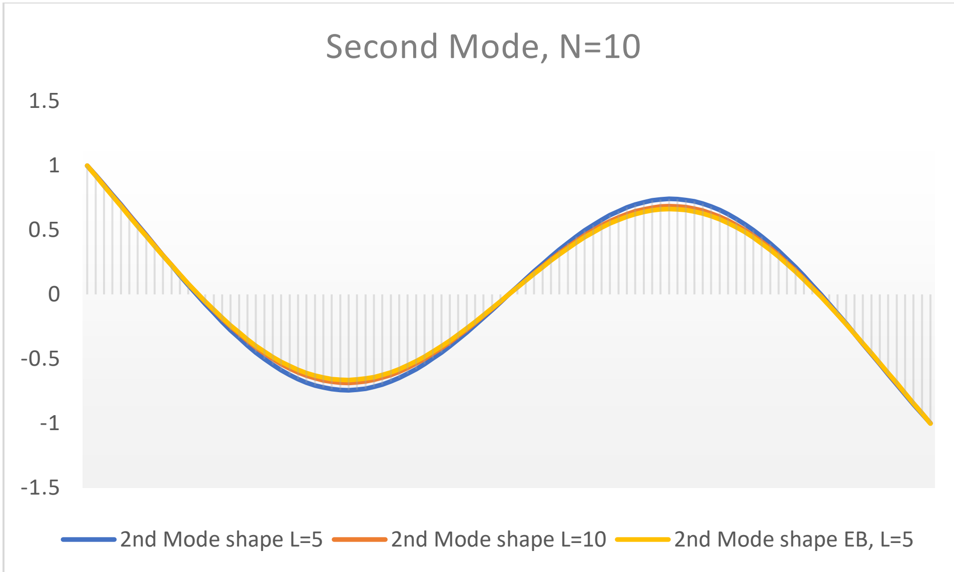

Figure A.2.2 Second mode shape for $L = 10$ and 5 compared with the Euler–Bernoulli mode shape for $N = 10$

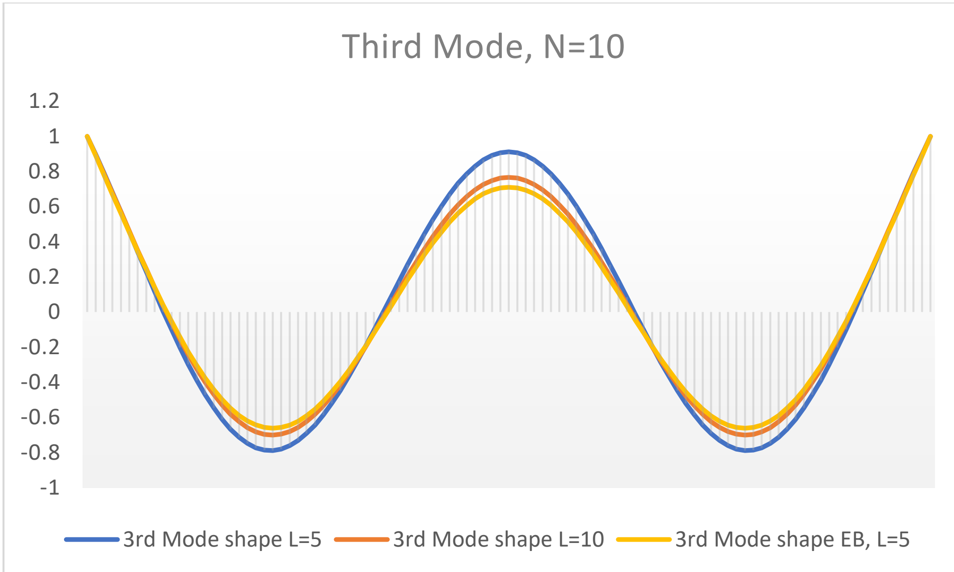

Figure A.2.3 Third mode shape for $L = 10$ and 5 compared with the Euler–Bernoulli mode shape for $N = 10$

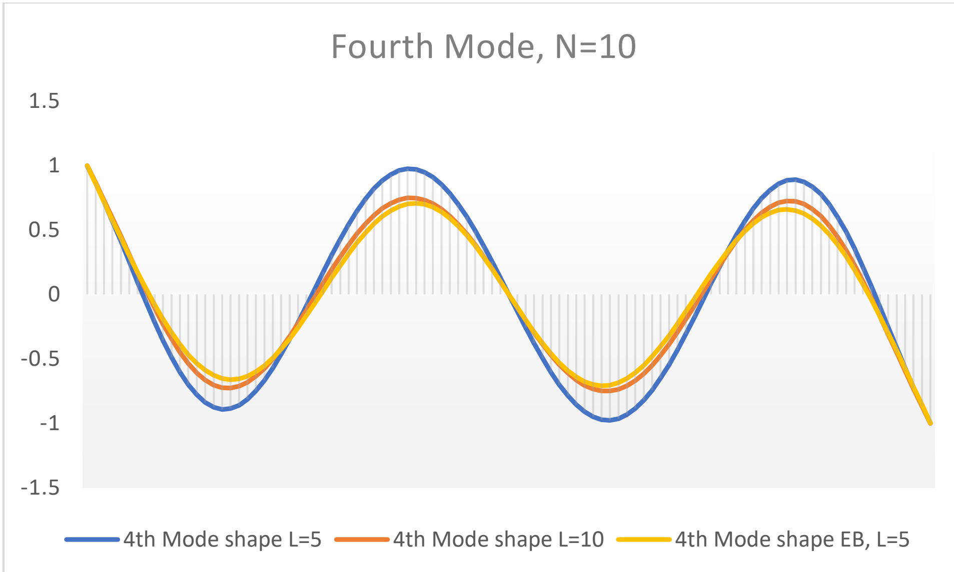

Figure A.2.4 Fourth mode shape for $L = 10$ and 5 compared with the Euler–Bernoulli mode shape for $N = 10$

A.3 The Mode Shapes of the Nonlinear Euler–Bernoulli Beam Theory

The figures presented in this section refer to the one-dimensional beam model of nonlinear Euler–Bernoulli theory; they have various boundary conditions.

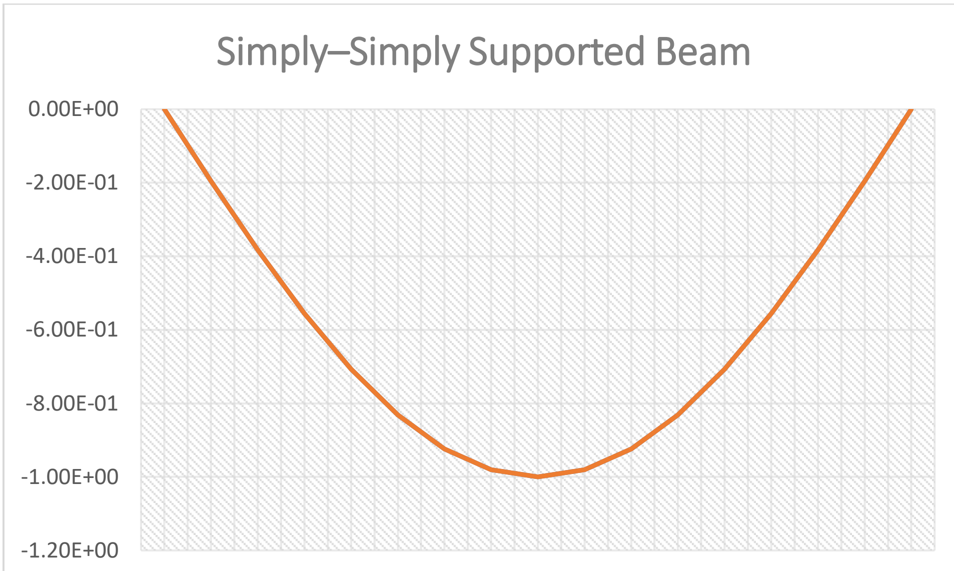

Figure A.3.1 First mode shape from nonlinear Euler–Bernoulli theory for a S–S beam

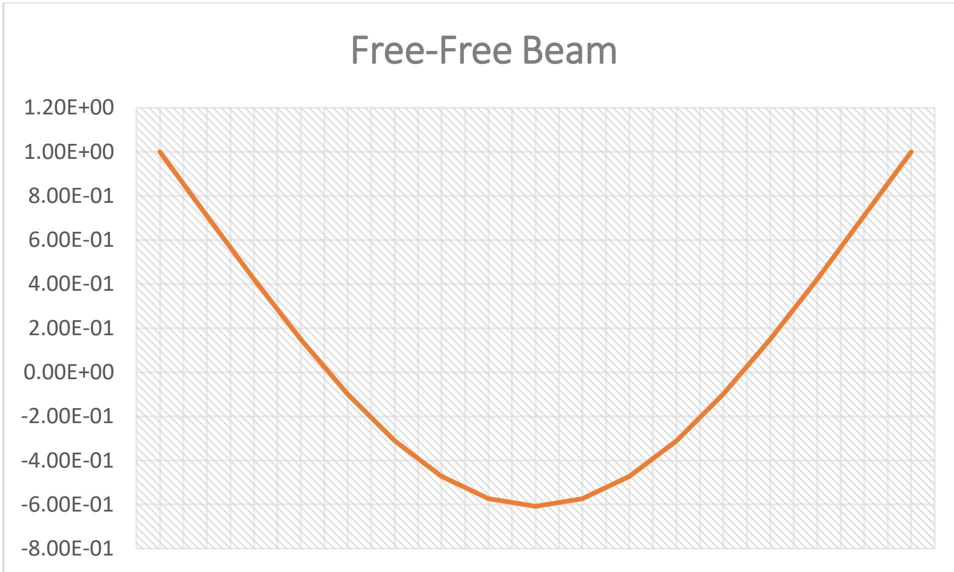

Figure A.3.2 First mode shape from nonlinear Euler–Bernoulli theory for a F–F beam

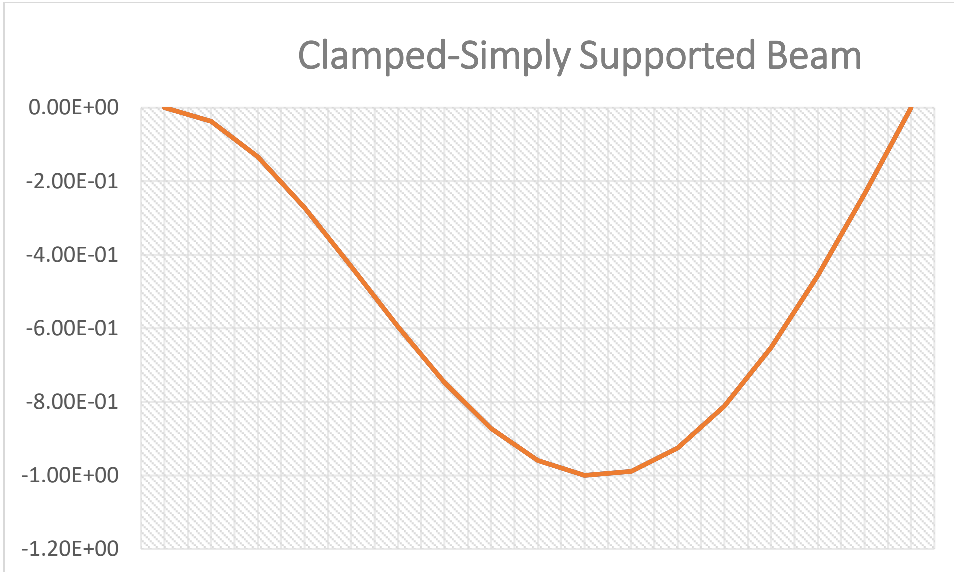

Figure A.3.3 First mode shape from nonlinear Euler–Bernoulli theory for a C–S beam

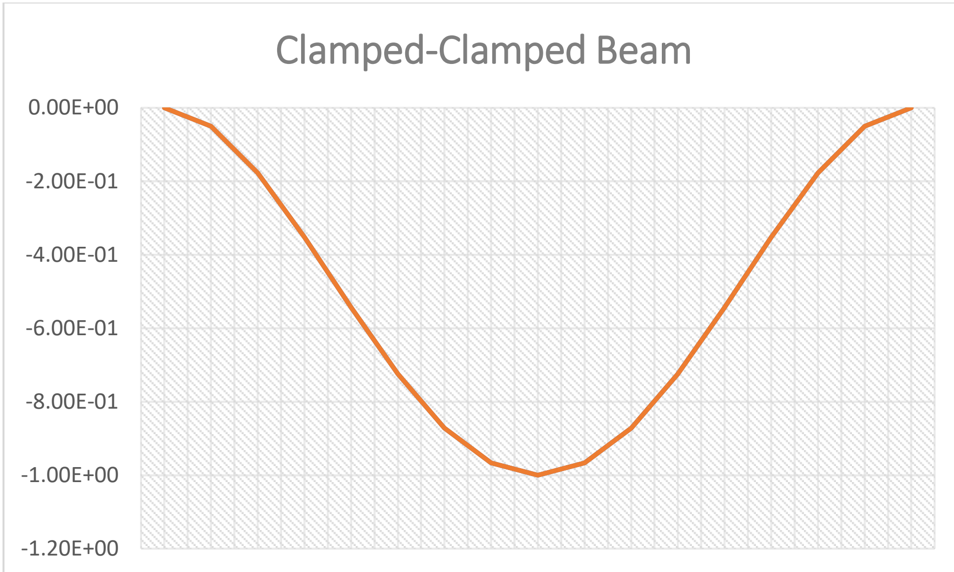

Figure A.3.4 First mode shape from nonlinear Euler–Bernoulli theory for a C–C beam

Table A.1 Linear natural frequency of E–B theory for S–S and F–F beams ($a/r = 1.0$)

Simply–Simply Supported Beam			Free–Free Beam		
$a/r = 1.0$			$a/r = 1.0$		
4 elements	8 elements	16 elements	4 elements	8 elements	16 elements
0.0016	0.0016	0.0016	0.0000	0.0000	0.0000
0.0262	0.0260	0.0260	0.0000	0.0000	0.0000
0.1364	0.1318	0.1315	0.0000	0.0000	0.0000
0.2077	0.1999	0.1980	0.0084	0.0083	0.0083
0.5120	0.4189	0.4158	0.0642	0.0635	0.0634
0.9600	0.8309	0.7998	0.2077	0.1999	0.1980
1.2936	1.0336	1.0160	0.2475	0.2447	0.2437
2.5351	1.9898	1.8285	0.8310	0.6729	0.6663
3.2349	2.1816	2.1095	0.9600	0.8309	0.7998
7.2605	3.8400	3.3237	2.0373	1.5175	1.4882
10.7520	4.1446	3.9163	2.5351	1.9898	1.8285
100.0000	6.5658	5.3424	3.8400	2.9988	2.9078
100.0000	8.1920	6.7024	4.9004	3.8400	3.3237
100.0000	10.1405	7.9591	13.5890	5.2776	5.1667
100.0000	12.6982	10.7844	16.5642	6.5658	5.3424

Table A.2 Nonlinear natural frequency of E–B theory for S–S and F–F beams ($a/r = 1.0$)

Simply–Simply Supported Beam			Free–Free Beam		
$a/r = 1.0$			$a/r = 1.0$		
4 elements	8 elements	16 elements	4 elements	8 elements	16 elements
0.0021	0.0020	0.0020	0.0000	0.0000	0.0000
0.0264	0.0260	0.0259	0.0000	0.0000	0.0000
0.1380	0.1319	0.1312	0.0001	0.0000	0.0000
0.2086	0.2009	0.1990	0.0086	0.0083	0.0083
0.5181	0.4192	0.4150	0.0651	0.0635	0.0631
0.9608	0.8332	0.8021	0.2101	0.2018	0.1995
1.3053	1.0343	1.0140	0.2523	0.2456	0.2435
2.5311	1.9941	1.8333	0.8419	0.6735	0.6620
3.2553	2.1830	2.1052	0.9791	0.8370	0.8070
7.2917	3.8469	3.3324	2.0730	1.5191	1.4796
10.7795	4.1506	3.9078	2.5772	2.0009	1.8424
100.0000	6.5749	5.3567	3.8593	2.9949	2.8891
100.0000	8.2173	6.6858	4.9710	3.8573	3.3502
100.0000	10.1423	7.9816	13.8109	5.2690	5.1127

Table A.3 Linear natural frequency of E–B theory for C–C and C–H beams ($a/r = 1.0$)

Clamped–Clamped Beam			Clamped–Hinged Beam		
$a/r = 1.0$			$a/r = 1.0$		
4 elements	8 elements	16 elements	4 elements	8 elements	16 elements
0.0084	0.0083	0.0083	0.0040	0.0040	0.0040
0.0646	0.0635	0.0634	0.0421	0.0416	0.0416
0.2077	0.1999	0.1980	0.1894	0.1818	0.1812
0.2541	0.2448	0.2437	0.2077	0.1999	0.1980
0.9097	0.6741	0.6663	0.6678	0.5350	0.5300
0.9600	0.8309	0.7998	0.9600	0.8309	0.7998
2.4882	1.5248	1.4883	1.7752	1.2609	1.2352
2.5351	1.9898	1.8285	2.5351	1.9898	1.8285
6.4596	3.0301	2.9083	4.5254	2.5806	2.4847
100.00	3.8400	3.3237	9.4852	3.8400	3.3237
100.00	5.3629	5.1686	100.00	4.7582	4.5096
100.00	6.5658	5.3424	100.00	6.5658	5.3424
100.00	10.1405	7.9591	100.00	9.2059	7.5879
100.00	10.6854	8.5597	100.00	10.1405	7.9591
100.00	13.7302	11.2646	100.00	13.7302	11.2646

Table A.4 Nonlinear natural frequency of E–B theory for C–C and C–H beams ($a/r = 1.0$)

Clamped–Clamped Beam			Clamped–Hinged Beam		
$a/r = 1.0$			$a/r = 1.0$		
4 elements	8 elements	16 elements	4 elements	8 elements	16 elements
0.0091	0.0089	0.0089	0.0046	0.0045	0.0045
0.0647	0.0635	0.0632	0.0427	0.0417	0.0415
0.2083	0.2003	0.1984	0.1899	0.1808	0.1797
0.2547	0.2452	0.2434	0.2098	0.2020	0.2001
0.9157	0.6749	0.6653	0.6751	0.5352	0.5287
0.9633	0.8328	0.8017	0.9623	0.8337	0.8026
2.5041	1.5264	1.4854	1.7895	1.2618	1.2323
2.5367	1.9943	1.8334	2.5348	1.9951	1.8344
6.4788	3.0263	2.9010	4.5516	2.5823	2.4783
100.00	3.8487	3.3338	9.5222	3.8487	3.3346
100.00	5.3502	5.1519	100.00	4.7582	4.4962
100.00	6.5802	5.3608	100.00	6.5780	5.3609
100.00	10.1753	7.9913	100.00	9.2252	7.5592
100.00	10.6997	8.5214	100.00	10.1665	7.9905
100.00	13.7470	11.3232	100.00	13.7331	11.3099

Table A.5 Linear natural frequency of E–B theory for S–S and F–F beams ($a/r = 0.4$)

Simply–Simply Supported Beam			Free–Free Beam		
$a/r = 0.4$			$a/r = 0.4$		
4 elements	8 elements	16 elements	4 elements	8 elements	16 elements
0.0016	0.0016	0.0016	0.0000	0.0000	0.0000
0.0262	0.0260	0.0260	0.0000	0.0000	0.0000
0.1364	0.1318	0.1315	0.0000	0.0000	0.0000
0.2077	0.1999	0.1980	0.0084	0.0083	0.0083
0.5120	0.4189	0.4158	0.0642	0.0635	0.0634
0.9600	0.8309	0.7998	0.2077	0.1999	0.1980
1.2936	1.0336	1.0160	0.2475	0.2447	0.2437
2.5351	1.9898	1.8285	0.8310	0.6729	0.6663
3.2349	2.1816	2.1095	0.9600	0.8309	0.7998
7.2605	3.8400	3.3237	2.0373	1.5175	1.4882
10.7520	4.1446	3.9163	2.5351	1.9898	1.8285
100.0000	6.5658	5.3424	3.8400	2.9988	2.9078
100.0000	8.1920	6.7024	4.9004	3.8400	3.3237
100.0000	10.1405	7.9591	13.5890	5.2776	5.1667
100.0000	12.6982	10.7844	16.5642	6.5658	5.3424

Table A.6 Nonlinear natural frequency of E–B theory for S–S and F–F beams ($a/r = 0.4$)

Simply–Simply Supported Beam			Free–Free Beam		
$a/r = 0.4$			$a/r = 0.4$		
4 elements	8 elements	16 elements	4 elements	8 elements	16 elements
0.0017	0.0017	0.0017	0.0000	0.0000	0.0000
0.0262	0.0260	0.0260	0.0000	0.0000	0.0000
0.1366	0.1318	0.1315	0.0000	0.0000	0.0000
0.2079	0.2001	0.1982	0.0084	0.0083	0.0083
0.5130	0.4189	0.4157	0.0643	0.0635	0.0633
0.9601	0.8313	0.8001	0.2081	0.2002	0.1983
1.2955	1.0337	1.0156	0.2483	0.2448	0.2437
2.5345	1.9905	1.8292	0.8328	0.6730	0.6656
3.2382	2.1819	2.1088	0.9630	0.8319	0.8009
7.2655	3.8411	3.3251	2.0432	1.5178	1.4868
10.7564	4.1455	3.9150	2.5417	1.9915	1.8307
100.00	6.5673	5.3447	3.8431	2.9982	2.9047
100.00	8.1961	6.6997	4.9117	3.8428	3.3280
100.00	10.1407	7.9627	13.6245	5.2762	5.1562
100.00	12.7057	10.7791	16.5971	6.5693	5.3543

Table A.7 Linear natural frequency of E–B theory for C–C and C–H beams ($a/r = 0.4$)

Clamped–Clamped Beam			Clamped–Hinged Beam		
$a/r = 0.4$			$a/r = 0.4$		
4 elements	8 elements	16 elements	4 elements	8 elements	16 elements
0.0084	0.0083	0.0083	0.0040	0.0040	0.0040
0.0646	0.0635	0.0634	0.0421	0.0416	0.0416
0.2077	0.1999	0.1980	0.1894	0.1818	0.1812
0.2541	0.2448	0.2437	0.2077	0.1999	0.1980
0.9097	0.6741	0.6663	0.6678	0.5350	0.5300
0.9600	0.8309	0.7998	0.9600	0.8309	0.7998
2.4882	1.5248	1.4883	1.7752	1.2609	1.2352
2.5351	1.9898	1.8285	2.5351	1.9898	1.8285
6.4596	3.0301	2.9083	4.5254	2.5806	2.4847
100.00	3.8400	3.3237	9.4852	3.8400	3.3237
100.00	5.3629	5.1686	100.00	4.7582	4.5096
100.00	6.5658	5.3424	100.00	6.5658	5.3424
100.00	10.1405	7.9591	100.00	9.2059	7.5879
100.00	10.6854	8.5597	100.00	10.1405	7.9591
100.00	13.7302	11.2646	100.00	13.7302	11.2646

Table A.8 Nonlinear natural frequency of E–B theory for C–C and C–H beams ($a/r = 0.4$)

Clamped–Clamped Beam			Clamped–Hinged Beam		
$a/r = 0.4$			$a/r = 0.4$		
4 elements	8 elements	16 elements	4 elements	8 elements	16 elements
0.0085	0.0084	0.0084	0.0041	0.0041	0.0040
0.0646	0.0635	0.0634	0.0422	0.0416	0.0416
0.2078	0.2000	0.1981	0.1895	0.1816	0.1809
0.2542	0.2448	0.2437	0.2081	0.2003	0.1984
0.9106	0.6742	0.6661	0.6690	0.5350	0.5298
0.9605	0.8312	0.8001	0.9604	0.8314	0.8002
2.4907	1.5250	1.4878	1.7775	1.2611	1.2347
2.5354	1.9905	1.8293	2.5351	1.9906	1.8294
6.4627	3.0295	2.9071	4.5296	2.5809	2.4837
100.00	3.8414	3.3253	9.4911	3.8414	3.3255
100.00	5.3608	5.1659	100.00	4.7582	4.5075
100.00	6.5681	5.3454	100.00	6.5678	5.3454
100.00	10.1461	7.9643	100.00	9.2089	7.5832
100.00	10.6877	8.5534	100.00	10.1447	7.9642
100.00	13.7329	11.2741	100.00	13.7307	11.2719

Table A.9 Linear natural frequency when $\upsilon = 0$ and $\upsilon = 0.3$ for $L = 10$ and $L = 4$ of a C–C beam

$a/r = 1$				$a/r = 1$			
$N = 6$				$N = 4$			
$L = 10$		$L = 4$		$L = 10$		$L = 4$	
υ = 0	υ = 0.3	υ = 0	υ = 0.3	υ = 0	υ = 0.3	υ = 0	υ = 0.3
0.00763	0.01099	0.19907	0.25711	0.00853	0.01198	0.20333	0.26372
0.05378	0.07541	1.02448	1.19746	0.05965	0.08476	1.1109	1.35293
0.1381	0.16771	1.22869	1.42461	0.19739	0.27447	1.2337	1.82347
0.1431	0.18132	1.32955	1.81053	0.2055	0.29124	3.03278	3.52172
0.19659	0.28874	2.07395	2.407	0.78956	1.12394	4.93474	7.18986
0.36401	0.54664	2.82899	4.39415	1.10108	1.17379	7.07434	7.62127
0.45264	0.72602	2.85503	4.63855	1.7736	2.64513	11.085	12.1564
0.80845	1.00000	5.05284	7.21903	2.9056	3.38022	11.6695	15.2873
1.09786	1.16966	6.8616	7.57743	3.18586	4.77808	15.2624	17.7981
1.14161	1.24571	7.10324	9.81683	9.91611	10.2288	18.16	23.7374
1.45506	1.55534	8.92202	9.86309	10.1393	11.2606	19.4474	27.8845
2.95785	1.60303	11.8758	12.3833	10.9378	15.4904	19.6473	32.3925
4.49225	4.84385	17.1691	18.658	14.3842	15.513	20.194	32.9109
10.1349	6.70569	18.4866	25.412	17.1065	18.7282	25.826	34.1774
11.0214	10.2151	19.0419	25.9997	19.667	33.7278	27.4635	42.625
12.3445	11.3237	19.1404	28.1577	19.7391	34.4438	29.503	45.9228
15.3885	13.1067	19.9502	29.75	24.5179	40.5123	41.827	49.0104
19.3416	17.3638	21.8361	33.0355	24.7624	42.6435	42.9767	49.9149
19.457	28.3449	24.3158	35.8981	40.0816	44.5132	61.9757	73.235
19.7137	29.3876	27.8562	40.8502	61.2716	62.3137	67.7547	85.39
19.7846	32.7382	28.0766	45.1939	62.802	65.016	76.4739	114.017
22.464	33.3127	38.2657	45.8408	79.5285	138.749	79.5342	137.248
24.3093	34.3921	39.1086	49.5154	120.2	170.295	121.253	171.264
26.0748	36.7687	41.4997	56.1388	120.269	171.5	121.972	178.251
39.7931	40.5673	48.1646	61.1319	170.534	210.804	172.678	215.023
41.0369	41.5213	56.6427	68.2755	171.705	212.007	179.707	222.536
42.8502	44.4622	75.0559	91.7543	340.157	380.558	339.787	382.258
66.4959	47.162	75.7637	93.1819	340.349	595.583	340.868	596.353
71.0189	70.9156	78.4258	106.583	380.948	596.098	384.575	599.592
78.2612	78.6397	79.1337	113.397	760.57	1330.97	761.094	1331.73

Table A.10 Nonlinear natural frequency when $\upsilon = 0$ and $\upsilon = 0.3$ for $L = 10$ and $L = 4$ of a C–C beam ($a/r = 1.0$)

$a/r = 1$				$a/r = 1$			
$N = 6$				$N = 4$			
$L = 10$		$L = 4$		$L = 10$		$L = 4$	
$\upsilon = 0$	$\upsilon = 0.3$	$\upsilon = 0$	$\upsilon = 0.3$	$\upsilon = 0$	$\upsilon = 0.3$	$\upsilon = 0$	$\upsilon = 0.3$
0.00812	0.01175	0.21499	0.279259	0.00902	0.01278	0.21938	0.28724
0.05362	0.07434	0.97236	1.127736	0.0595	0.08387	1.03338	1.25177
0.13772	0.16688	1.27453	1.361043	0.19773	0.27404	1.31848	1.90904
0.14294	0.1792	1.33012	1.891309	0.20546	0.29156	2.96741	3.44127
0.19688	0.28902	1.99255	2.224437	0.79114	1.12335	5.04182	7.27582
0.33393	0.49027	2.39158	3.688728	1.09808	1.17429	6.9218	7.5027
0.48547	0.76949	3.34394	5.210609	1.78021	2.65207	11.1598	12.1426
0.81344	1.16871	5.13996	7.209201	2.79821	3.32279	11.8635	15.6053
1.0899	1.23678	6.87736	7.997688	3.31067	4.8692	15.0346	17.77
1.15087	1.59423	7.18441	9.121198	9.92076	10.2288	16.7626	21.236
1.46719	1.61522	8.86406	10.46113	10.1394	11.261	19.4811	31.1908
2.96239	4.85258	11.8467	12.36937	10.938	15.4762	19.6565	31.8129
4.50934	6.73073	17.0281	18.65132	14.3845	15.5376	21.9848	33.4669
10.1349	10.2151	18.6748	25.66501	17.1087	18.7316	25.6273	34.2358
11.0213	11.3235	19.0736	26.23572	19.668	33.7292	27.6104	42.8666
12.3441	13.1068	19.2278	27.99219	19.7397	34.4446	29.99	46.2913
15.3837	17.3591	20.0902	29.90813	24.5213	40.513	41.8369	47.1434
19.3361	28.2668	21.6951	32.99942	24.7709	42.6488	43.5094	52.4055
19.46	29.4661	24.4987	36.3738	40.0816	44.5257	62.1855	73.2847
19.7146	32.7416	28.0732	40.86027	61.2716	62.314	67.7595	85.4376
19.7855	33.3148	28.0844	43.61798	62.8022	65.0169	76.4955	114.339
22.4686	34.3933	35.813	45.99725	79.5289	138.75	79.5529	137.277
24.3199	36.7787	41.5041	49.57926	120.201	170.295	121.291	171.266
26.0962	40.5682	41.6505	56.08789	120.272	171.5	122.083	178.268
39.7931	41.5339	48.4723	63.02847	170.534	210.806	172.679	215.089
41.037	44.4818	56.5525	68.19985	171.705	212.013	179.715	222.717
42.8507	47.1692	75.406	91.75829	340.158	380.558	339.818	382.258
66.4965	70.92	75.8258	93.16726	340.349	595.584	340.885	596.383
71.0179	78.6399	78.4603	107.056	380.948	596.099	384.577	599.653
78.2636	91.3188	79.1842	113.704	760.571	1330.97	761.111	1331.76

Table A.11 Linear natural frequency when $\upsilon = 0$ and $\upsilon = 0.3$ for $L = 20$ and $L = 40$ of a C–C beam ($a/r = 1$)

$a/r = 1.0$				$a/r = 1.0$			
$N = 6$				$N = 4$			
$L = 20$		$L = 40$		$L = 20$		$L = 40$	
$\upsilon = 0$	$\upsilon = 0.3$	$\upsilon = 0$	$\upsilon = 0.3$	$\upsilon = 0$	$\upsilon = 0.3$	$\upsilon = 0$	$\upsilon = 0.3$
0.00051	0.00076	3.3E-05	4.9E-05	0.00071	0.00096	5.7E-05	7.8E-05
0.00397	0.0059	0.00026	0.00039	0.00576	0.00794	0.00075	0.0009
0.01131	0.01602	0.00077	0.00112	0.02185	0.02919	0.00297	0.00351
0.01639	0.02247	0.00128	0.00194	0.04935	0.07278	0.01234	0.01819
0.04915	0.07217	0.00618	0.00952	0.19739	0.27478	0.04935	0.06826
0.05718	0.08567	0.01229	0.01804	0.2732	0.29418	0.06816	0.07359
0.11316	0.18079	0.02829	0.04515	0.4434	0.66612	0.11085	0.16682
0.20211	0.25052	0.05053	0.05604	0.7264	0.81981	0.1816	0.20306
0.23793	0.29256	0.05508	0.07314	0.80627	1.20007	0.20219	0.30033
0.27446	0.40214	0.06862	0.10063	2.47903	4.00124	0.61976	1.00595
0.57288	0.61276	0.18487	0.30498	9.94085	9.96337	9.89153	9.89716
0.73946	1.21831	0.28077	0.3301	10.1398	10.2244	9.94127	9.96269
1.12306	1.70985	0.31717	0.42921	12.6076	12.8982	12.1527	12.2261
9.93556	9.95561	9.88612	9.89109	13.2988	13.7472	12.3267	12.4425
10.1585	10.2389	9.94223	9.96338	19.7318	34.3151	19.7459	34.498
10.5101	10.7061	10.0364	10.0849	19.7483	34.5321	19.7498	34.5551
11.8156	12.3211	10.8962	11.0228	24.1273	39.9752	24.0317	39.8207
14.6754	16.1781	12.6743	13.0551	24.1801	42.1437	24.0442	42.0348
19.6103	30.4698	19.7095	30.7088	39.8438	42.4591	39.7846	42.1044
19.6792	33.8876	19.73	34.3675	60.3192	60.5903	60.0799	60.1484
19.73	34.0817	19.738	34.4137	60.7089	61.3054	60.1778	60.3305
19.7411	34.4964	19.7441	34.5347	79.5294	139.064	79.5296	139.148
24.0587	37.2361	24.0132	37.9159	120.05	170.167	120.013	170.135
24.4712	39.7803	24.1131	39.5591	120.065	170.473	120.016	170.212
39.5583	40.4827	39.4994	39.991	170.227	210.201	170.15	210.05
40.083	42.2319	39.8444	40.8639	170.522	210.502	170.224	210.126
40.5714	42.6491	39.9694	42.0031	340.226	380.316	340.244	380.255
61.6608	63.03	60.4179	60.7878	340.275	595.474	340.256	595.446
62.7964	64.9133	60.7022	61.2542	380.414	595.602	380.28	595.479
78.8608	91.1649	78.9415	91.0343	760.495	1330.86	760.477	1330.83

Table A.12 Nonlinear natural frequency when $\upsilon = 0$ and $\upsilon = 0.3$ for $L = 20$ and $L = 40$ of a C–C beam ($a/r = 1.0$)

$a/r = 1.0$				$a/r = 1.0$			
$N = 6$				$N = 4$			
$L = 20$		$L = 40$		$L = 20$		$L = 40$	
$\upsilon = 0$	$\upsilon = 0.3$	$\upsilon = 0$	$\upsilon = 0.3$	$\upsilon = 0$	$\upsilon = 0.3$	$\upsilon = 0$	$\upsilon = 0.3$
0.00396	0.00585	0.00026	0.00039	0.00074	0.00102	6E-05	8.2E-05
0.01131	0.01597	0.00077	0.00112	0.00576	0.00791	0.00075	0.0009
0.01639	0.02241	0.00128	0.00193	0.02189	0.02921	0.00297	0.00351
0.04916	0.07216	0.00613	0.00919	0.04935	0.07277	0.01234	0.01819
0.05547	0.08091	0.01229	0.01804	0.19748	0.27483	0.04935	0.06827
0.11549	0.184	0.02844	0.04536	0.27309	0.29414	0.06816	0.07358
0.20256	0.25036	0.05056	0.05604	0.44373	0.66648	0.11086	0.16683
0.2378	0.29254	0.05508	0.07314	0.71799	0.81646	0.18103	0.20288
0.27472	0.40263	0.06863	0.10065	0.81603	1.20597	0.20286	0.30071
0.57453	0.61802	0.18488	0.30501	2.47938	4.00189	0.61978	1.006
0.7397	1.21831	0.27498	0.32573	9.94085	9.96337	9.89153	9.89716
1.13062	1.70985	0.32537	0.43786	10.1398	10.2244	9.94127	9.96269
9.93556	9.95561	9.88612	9.89109	12.6076	12.8983	12.1527	12.2261
10.1585	10.2389	9.94223	9.96338	13.2988	13.7473	12.3267	12.4425
10.5101	10.7061	10.0364	10.0849	19.7319	34.3152	19.7459	34.498
11.8157	12.3211	10.8962	11.0228	19.7484	34.5322	19.7498	34.5551
14.6753	16.1781	12.6743	13.0551	24.1275	1.20007	24.0317	39.8207
19.6108	30.4698	19.7096	30.7088	24.1801	4.00124	24.0442	42.0348
19.6794	33.8876	19.73	34.3675	39.8438	9.96337	39.7846	42.1044
19.7302	34.0817	19.7381	34.4137	60.3192	10.2244	60.0799	60.1484
19.7412	34.4964	19.7441	34.5347	60.7089	12.8982	60.1778	60.3305
24.0589	37.2361	24.0132	37.9159	79.5294	13.7472	79.5296	139.148
24.4724	39.7803	24.1132	39.5591	120.05	34.3151	120.013	170.135
39.5583	40.4827	39.4994	39.991	120.065	34.5321	120.016	170.212
40.083	42.2319	39.8444	40.8639	170.227	39.9752	170.15	210.05
40.5714	42.6491	39.9694	42.0031	170.522	42.1437	170.224	210.126
61.6608	63.03	60.4179	60.7878	340.226	42.4591	340.244	380.255
62.7963	64.9133	60.7022	61.2542	340.275	60.5903	340.256	595.446
78.8609	91.1649	78.9415	91.0343	380.414	61.3054	380.28	595.479
79.3117	91.249	79.4594	91.2314	760.495	139.064	760.477	1330.83

Table A.13 Linear natural frequency when $\upsilon = 0$ and $\upsilon = 0.3$ for $L = 10$ and $L = 4$ of a C–C beam ($a/r = 1.5$)

$a/r = 1.5$				$a/r = 1.5$			
$N = 6$				$N = 4$			
$L = 10$		$L = 4$		$L = 10$		$L = 4$	
$\upsilon = 0$	$\upsilon = 0.3$	$\upsilon = 0$	$\upsilon = 0.3$	$\upsilon = 0$	$\upsilon = 0.3$	$\upsilon = 0$	$\upsilon = 0.3$
0.00763	0.01099	0.19907	0.25711	0.00853	0.01198	0.20333	0.26372
0.05378	0.07541	1.02448	1.19746	0.05965	0.08476	1.1109	1.35293
0.1381	0.16771	1.22869	1.42461	0.19739	0.27447	1.2337	1.82347
0.1431	0.18132	1.32955	1.81053	0.2055	0.29124	3.03278	3.52172
0.19659	0.28874	2.07395	2.407	0.78956	1.12394	4.93474	7.18986
0.36401	0.54664	2.82899	4.39415	1.10108	1.17379	7.07434	7.62127
0.45264	0.72602	2.85503	4.63855	1.7736	2.64513	11.085	12.1564
0.80845	1.16966	5.05284	7.21903	2.9056	3.38022	11.6695	15.2873
1.09786	1.24571	6.8616	7.57743	3.18586	4.77808	15.2624	17.7981
1.14161	1.55534	7.10324	9.81683	9.91611	10.2288	18.16	23.7374
1.45506	1.60303	8.92202	9.86309	10.1393	11.2606	19.4474	27.8845
2.95785	4.84385	11.8758	12.3833	10.9378	15.4904	19.6473	32.3925
4.49225	6.70569	17.1691	18.658	14.3842	15.513	20.194	32.9109
10.1349	10.2151	18.4866	25.412	17.1065	18.7282	25.826	34.1774
11.0214	11.3237	19.0419	25.9997	19.667	33.7278	27.4635	42.625
12.3445	13.1067	19.1404	28.1577	19.7391	34.4438	29.503	45.9228
15.3885	17.3638	19.9502	29.75	24.5179	40.5123	41.827	49.0104
19.3416	28.3449	21.8361	33.0355	24.7624	42.6435	42.9767	49.9149
19.457	29.3876	24.3158	35.8981	40.0816	44.5132	61.9757	73.235
19.7137	32.7382	27.8562	40.8502	61.2716	62.3137	67.7547	85.39
19.7846	33.3127	28.0766	45.1939	62.802	65.016	76.4739	114.017
22.464	34.3921	38.2657	45.8408	79.5285	138.749	79.5342	137.248
24.3093	36.7687	39.1086	49.5154	120.2	170.295	121.253	171.264
26.0748	40.5673	41.4997	56.1388	120.269	171.5	121.972	178.251
39.7931	41.5213	48.1646	61.1319	170.534	210.804	172.678	215.023
41.0369	44.4622	56.6427	68.2755	171.705	212.007	179.707	222.536
42.8502	47.162	75.0559	91.7543	340.157	380.558	339.787	382.258
66.4959	70.9156	75.7637	93.1819	340.349	595.583	340.868	596.353
71.0189	78.6397	78.4258	106.583	380.948	596.098	384.575	599.592
78.2612	91.3188	79.1337	113.397	760.57	1330.97	761.094	1331.73

Table A.14 Nonlinear natural frequency when $\upsilon = 0$ and $\upsilon = 0.3$ for $L = 10$ and $L = 4$ of a C–C beam ($a/r = 1.5$)

$a/r = 1.5$				$a/r = 1.5$			
$N = 6$				$N = 4$			
$L = 10$		$L = 4$		$L = 10$		$L = 4$	
$\upsilon = 0$	$\upsilon = 0.3$	$\upsilon = 0$	$\upsilon = 0.3$	$\upsilon = 0$	$\upsilon = 0.3$	$\upsilon = 0$	$\upsilon = 0.3$
0.00873	0.01269	0.23465	0.30603	0.00963	0.01377	0.23925	0.31604
0.05342	0.07301	0.92651	1.04384	0.05931	0.08276	0.97848	1.15711
0.13725	0.16583	1.2904	1.3115	0.19815	0.2735	1.38227	1.98388
0.14274	0.17658	1.35301	1.95874	0.20541	0.29195	2.89552	3.35006
0.19723	0.28934	1.89186	2.02702	0.79311	1.12265	5.16387	7.36186
0.31012	0.441	2.2078	3.28291	1.09441	1.17486	6.75541	7.36977
0.5124	0.80358	3.58799	5.39116	1.78838	2.66071	11.2025	12.1284
0.81955	1.16829	5.24764	7.36873	2.71414	3.25987	12.1312	15.9841
1.0826	1.22648	6.89301	8.38086	3.4165	4.97423	14.5895	17.7127
1.1598	1.62959	7.28753	8.72166	9.92657	10.2288	16.1331	19.7004
1.48246	1.64061	8.80118	10.7548	10.1395	11.2615	19.5213	31.4282
2.96805	4.8635	11.8157	12.3603	10.9384	15.4681	19.6769	33.4825
4.53072	6.76182	16.8775	18.6439	14.3848	15.5587	23.2023	33.8315
10.1349	10.2151	18.8363	25.8197	17.1114	18.7359	25.4377	34.5502
11.0212	11.3234	19.1456	26.5248	19.6692	33.731	27.8304	43.1059
12.3437	13.1069	19.3032	27.9006	19.7404	34.4457	30.5409	46.1884
15.3777	17.3532	20.273	30.1701	24.5254	40.5137	41.8501	46.8027
19.3293	28.182	21.591	32.9468	24.7816	42.6555	44.1962	54.1794
19.4637	29.5515	24.6846	36.9167	40.0816	44.5412	62.449	73.3509
19.7156	32.7458	28.1008	40.8718	61.2716	62.3142	67.7655	85.4986
19.7868	33.3175	28.3447	42.1674	62.8024	65.0181	76.5231	114.742
22.4742	34.3949	34.5048	46.2028	79.5294	138.751	79.5764	137.314
24.3332	36.7913	41.5096	49.5258	120.202	170.295	121.338	171.268
26.123	40.5693	42.9709	55.9658	120.275	171.5	122.221	178.288
39.7931	41.5493	48.9479	65.09	170.534	210.807	172.68	215.171
41.0372	44.5065	56.4437	68.1074	171.705	212.019	179.726	222.943
42.8514	47.1783	75.8393	91.7632	340.159	380.558	339.858	382.258
66.4972	70.9255	75.9019	93.1491	340.35	595.585	340.907	596.42
71.0167	78.6402	78.5038	107.64	380.948	596.101	384.58	599.731
78.2665	91.3188	79.2475	114.119	760.571	1330.97	761.133	1331.79

Table A.15 Linear natural frequency when $\upsilon = 0$ and $\upsilon = 0.3$ for $L = 20$ and $L = 40$ of a C–C beam ($a/r = 1.5$)

$a/r = 1.5$				$a/r = 1.5$			
$N = 6$				$N = 4$			
$L = 20$		$L = 40$		$L = 20$		$L = 40$	
$\upsilon = 0$	$\upsilon = 0.3$	$\upsilon = 0$	$\upsilon = 0.3$	$\upsilon = 0$	$\upsilon = 0.3$	$\upsilon = 0$	$\upsilon = 0.3$
0.00051	0.00076	3.3E-05	4.9E-05	0.00071	0.00096	5.7E-05	7.8E-05
0.00397	0.0059	0.00026	0.00039	0.00576	0.00794	0.00075	0.0009
0.01131	0.01602	0.00077	0.00112	0.02185	0.02919	0.00297	0.00351
0.01639	0.02247	0.00128	0.00194	0.04935	0.07278	0.01234	0.01819
0.04915	0.07217	0.00618	0.00952	0.19739	0.27478	0.04935	0.06826
0.05718	0.08567	0.01229	0.01804	0.2732	0.29418	0.06816	0.07359
0.11316	0.18079	0.02829	0.04515	0.4434	0.66612	0.11085	0.16682
0.20211	0.25052	0.05053	0.05604	0.7264	0.81981	0.1816	0.20306
0.23793	0.29256	0.05508	0.07314	0.80627	1.20007	0.20219	0.30033
0.27446	0.40214	0.06862	0.10063	2.47903	4.00124	0.61976	1.00595
0.57288	0.61276	0.18487	0.30498	9.94085	9.96337	9.89153	9.89716
0.73946	1.21831	0.28077	0.3301	10.1398	10.2244	9.94127	9.96269
1.12306	1.70985	0.31717	0.42921	12.6076	12.8982	12.1527	12.2261
9.93556	9.95561	9.88612	9.89109	13.2988	13.7472	12.3267	12.4425
10.1585	10.2389	9.94223	9.96338	19.7318	34.3151	19.7459	34.498
10.5101	10.7061	10.0364	10.0849	19.7483	34.5321	19.7498	34.5551
11.8156	12.3211	10.8962	11.0228	24.1273	39.9752	24.0317	39.8207
14.6754	16.1781	12.6743	13.0551	24.1801	42.1437	24.0442	42.0348
19.6103	30.4698	19.7095	30.7088	39.8438	42.4591	39.7846	42.1044
19.6792	33.8876	19.73	34.3675	60.3192	60.5903	60.0799	60.1484
19.73	34.0817	19.738	34.4137	60.7089	61.3054	60.1778	60.3305
19.7411	34.4964	19.7441	34.5347	79.5294	139.064	79.5296	139.148
24.0587	37.2361	24.0132	37.9159	120.05	170.167	120.013	170.135
24.4712	39.7803	24.1131	39.5591	120.065	170.473	120.016	170.212
39.5583	40.4827	39.4994	39.991	170.227	210.201	170.15	210.05
40.083	42.2319	39.8444	40.8639	170.522	210.502	170.224	210.126
40.5714	42.6491	39.9694	42.0031	340.226	380.316	340.244	380.255
61.6608	63.03	60.4179	60.7878	340.275	595.474	340.256	595.446
62.7964	64.9133	60.7022	61.2542	380.414	595.602	380.28	595.479
78.8608	91.1649	78.9415	91.0343	760.495	1330.86	760.477	1330.83

Table A.16 Nonlinear natural frequency when $\upsilon = 0$ and $\upsilon = 0.3$ for $L = 20$ and $L = 40$ of a C–C beam ($a/r = 1.5$)

$a/r = 1.5$				$a/r = 1.5$			
$N = 6$				$N = 4$			
$L = 20$		$L = 40$		$L = 20$		$L = 40$	
$\upsilon = 0$	$\upsilon = 0.3$	$\upsilon = 0$	$\upsilon = 0.3$	$\upsilon = 0$	$\upsilon = 0.3$	$\upsilon = 0$	$\upsilon = 0.3$
0.00059	0.00088	3.7E-05	5.6E-05	0.00079	0.0011	6.4E-05	8.8E-05
0.00396	0.00579	0.00026	0.00039	0.00576	0.00786	0.00075	0.0009
0.01132	0.0159	0.00077	0.00112	0.02193	0.02923	0.00298	0.00351
0.01638	0.02232	0.00128	0.00193	0.04936	0.07276	0.01234	0.01819
0.04917	0.07214	0.00606	0.00879	0.19758	0.27488	0.04936	0.06828
0.05355	0.07553	0.01229	0.01804	0.27295	0.29409	0.06816	0.07357
0.11813	0.1875	0.02862	0.04561	0.44413	0.66693	0.11088	0.16685
0.20312	0.25017	0.0506	0.05604	0.70942	0.81242	0.18036	0.20265
0.23765	0.29253	0.05508	0.07314	0.82629	1.2132	0.20365	0.30117
0.27503	0.40323	0.06864	0.10069	2.47981	4.0027	0.61981	1.00605
0.57655	0.62438	0.1849	0.30504	9.94085	9.96337	9.89153	9.89716
0.7400	1.21934	0.26978	0.32111	10.1398	10.2244	9.94127	9.96269
1.14013	1.73791	0.3336	0.44781	12.6076	12.8983	12.1527	12.2261
9.93556	9.95561	9.88612	9.89109	13.2989	13.7473	12.3267	12.4425
10.1585	10.2389	9.94223	9.96338	19.7319	34.3153	19.7459	34.498
10.5101	10.7062	10.0364	10.0849	19.7484	34.5322	19.7498	34.5551
11.8157	12.3214	10.8962	11.0229	24.1277	39.9753	24.0317	39.8207
14.6751	16.1777	12.6743	13.0551	24.1813	42.1445	24.0443	42.0348
19.6114	30.4711	19.7096	30.7089	39.8438	42.461	39.7846	42.1046
19.6796	33.8882	19.73	34.3675	60.3192	60.5903	60.0799	60.1484
19.7304	34.0819	19.7381	34.4137	60.7089	61.3054	60.1778	60.3305
19.7412	34.4966	19.7442	34.5347	79.5294	139.064	79.5296	139.148
24.0591	37.2371	24.0132	37.916	120.05	170.167	120.013	170.135
24.4739	39.7803	24.1133	39.5591	120.066	170.473	120.016	170.212
39.5583	40.4832	39.4994	39.991	170.227	210.201	170.15	210.05
40.083	42.2359	39.8444	40.8639	170.522	210.503	170.224	210.126
40.5714	42.6498	39.9694	42.0033	340.226	380.316	340.244	380.255
61.6608	63.0303	60.4179	60.7878	340.275	595.474	340.256	595.446
62.7963	64.9133	60.7022	61.2542	380.414	595.603	380.28	595.479
78.861	91.1654	78.9415	91.0347	760.495	1330.86	760.477	1330.83

Table A.17 Linear natural frequency when $\upsilon = 0$ and $\upsilon = 0.3$ for $L = 10$ and $L = 4$ of a C–C beam ($a/r = 2.0$)

$a/r = 2$				$a/r = 2$			
$N = 6$				$N = 4$			
$L = 10$		$L = 4$		$L = 10$		$L = 4$	
$\upsilon = 0$	$\upsilon = 0.3$	$\upsilon = 0$	$\upsilon = 0.3$	$\upsilon = 0$	$\upsilon = 0.3$	$\upsilon = 0$	$\upsilon = 0.3$
0.00763	0.01099	0.19907	0.25711	0.00853	0.01198	0.20333	0.26372
0.05378	0.07541	1.02448	1.19746	0.05965	0.08476	1.1109	1.35293
0.1381	0.16771	1.22869	1.42461	0.19739	0.27447	1.2337	1.82347
0.1431	0.18132	1.32955	1.81053	0.2055	0.29124	3.03278	3.52172
0.19659	0.28874	2.07395	2.407	0.78956	1.12394	4.93474	7.18986
0.36401	0.54664	2.82899	4.39415	1.10108	1.17379	7.07434	7.62127
0.45264	0.72602	2.85503	4.63855	1.7736	2.64513	11.085	12.1564
0.80845	1.16966	5.05284	7.21903	2.9056	3.38022	11.6695	15.2873
1.09786	1.24571	6.8616	7.57743	3.18586	4.77808	15.2624	17.7981
1.14161	1.55534	7.10324	9.81683	9.91611	10.2288	18.16	23.7374
1.45506	1.60303	8.92202	9.86309	10.1393	11.2606	19.4474	27.8845
2.95785	4.84385	11.8758	12.3833	10.9378	15.4904	19.6473	32.3925
4.49225	6.70569	17.1691	18.658	14.3842	15.513	20.194	32.9109
10.1349	10.2151	18.4866	25.412	17.1065	18.7282	25.826	34.1774
11.0214	11.3237	19.0419	25.9997	19.667	33.7278	27.4635	42.625
12.3445	13.1067	19.1404	28.1577	19.7391	34.4438	29.503	45.9228
15.3885	17.3638	19.9502	29.75	24.5179	40.5123	41.827	49.0104
19.3416	28.3449	21.8361	33.0355	24.7624	42.6435	42.9767	49.9149
19.457	29.3876	24.3158	35.8981	40.0816	44.5132	61.9757	73.235
19.7137	32.7382	27.8562	40.8502	61.2716	62.3137	67.7547	85.39
19.7846	33.3127	28.0766	45.1939	62.802	65.016	76.4739	114.017
22.464	34.3921	38.2657	45.8408	79.5285	138.749	79.5342	137.248
24.3093	36.7687	39.1086	49.5154	120.2	170.295	121.253	171.264
26.0748	40.5673	41.4997	56.1388	120.269	171.5	121.972	178.251
39.7931	41.5213	48.1646	61.1319	170.534	210.804	172.678	215.023
41.0369	44.4622	56.6427	68.2755	171.705	212.007	179.707	222.536
42.8502	47.162	75.0559	91.7543	340.157	380.558	339.787	382.258
66.4959	70.9156	75.7637	93.1819	340.349	595.583	340.868	596.353
71.0189	78.6397	78.4258	106.583	380.948	596.098	384.575	599.592
78.2612	91.3188	79.1337	113.397	760.57	1330.97	761.094	1331.73

Table A.18 Nonlinear natural frequency when $\upsilon = 0$ and $\upsilon = 0.3$ for $L = 10$ and $L = 4$ of a C–C beam ($a/r = 2.0$)

$a/r = 2$				$a/r = 2$			
$N = 6$				$N = 4$			
$L = 10$		$L = 4$		$L = 10$		$L = 4$	
$\upsilon = 0$	$\upsilon = 0.3$	$\upsilon = 0$	$\upsilon = 0.3$	$\upsilon = 0$	$\upsilon = 0.3$	$\upsilon = 0$	$\upsilon = 0.3$
0.00958	0.01397	0.26174	0.34159	0.01048	0.01514	0.26669	0.35516
0.05315	0.07117	0.87754	0.93852	0.05905	0.08124	0.92388	1.0527
0.13659	0.16435	1.28288	1.25856	0.19874	0.27277	1.44892	2.05987
0.14246	0.17298	1.39971	1.792	0.20535	0.29248	2.80856	3.23674
0.19773	0.28975	1.75896	2.02391	0.79585	1.12169	5.31704	7.2074
0.28626	0.38865	2.05558	2.8894	1.08944	1.17558	6.5559	7.44446
0.54009	0.83637	3.8092	5.41804	1.79965	2.67277	11.227	12.1124
0.82783	1.16875	5.39946	7.70433	2.62851	3.18381	12.5055	16.486
1.0747	1.21341	6.90707	8.30597	3.53258	5.10928	13.8733	17.5001
1.16999	1.64836	7.43349	8.81817	9.9347	10.2287	15.8222	18.5041
1.50395	1.70192	8.73037	11.0457	10.1397	11.2622	19.5741	31.0448
2.97598	4.87878	11.7799	12.3629	10.9388	15.461	19.7061	34.086
4.5607	6.80498	16.698	18.6347	14.3853	15.584	24.3175	34.2011
10.1349	10.2151	18.9243	25.7779	17.1153	18.742	25.2405	36.7159
11.021	11.3232	19.2992	26.9194	19.6709	33.7335	28.2169	43.354
12.343	13.1071	19.3759	27.9463	19.7413	34.4471	31.2455	45.3209
15.3693	17.345	20.5297	30.6338	24.5313	40.5148	41.8699	47.5864
19.3197	28.0789	21.5614	32.8572	24.7965	42.6648	45.1946	56.2664
19.4688	29.6554	24.8967	37.6084	40.0816	44.563	62.8202	73.4533
19.7171	32.7518	28.1356	40.6403	61.2717	62.3146	67.7742	85.5871
19.7887	33.3212	28.7232	40.8854	62.8026	65.0196	76.5626	115.31
22.4819	34.397	33.2741	46.51	79.5301	138.752	79.6092	137.366
24.3518	36.8089	41.5175	49.3892	120.203	170.295	121.405	171.271
26.1605	40.5708	44.0473	55.7995	120.281	171.5	122.415	178.317
39.7932	41.5706	49.7694	67.557	170.534	210.81	172.682	215.285
41.0374	44.5415	56.2981	67.9818	171.705	212.028	179.741	223.26
42.8524	47.1911	76.0058	91.7697	340.161	380.558	339.914	382.258
66.4982	70.9332	76.4377	93.1245	340.35	595.586	340.938	596.472
71.0151	78.6407	78.5658	108.443	380.948	596.104	384.584	599.839
78.2707	91.3188	79.3366	114.754	760.572	1330.97	761.163	1331.85

Table A.19 Linear natural frequency when $\upsilon = 0$ and $\upsilon = 0.3$ for $L = 20$ and $L = 40$ of a C–C beam ($a/r = 2.0$)

$a/r = 2$				$a/r = 2$			
$N = 6$				$N = 4$			
$L = 20$		$L = 40$		$L = 20$		$L = 40$	
$\upsilon = 0$	$\upsilon = 0.3$	$\upsilon = 0$	$\upsilon = 0.3$	$\upsilon = 0$	$\upsilon = 0.3$	$\upsilon = 0$	$\upsilon = 0.3$
0.000514	0.000761	3.28E-05	4.89E-05	0.000707	0.000963	5.73E-05	7.78E-05
0.003965	0.005902	0.00026	0.000394	0.005757	0.007944	0.000754	0.000904
0.011308	0.016022	0.000767	0.00112	0.021851	0.029194	0.002966	0.003506
0.016394	0.022472	0.001281	0.001936	0.049348	0.072783	0.012337	0.018194
0.049148	0.072171	0.006184	0.009516	0.19739	0.274782	0.049347	0.068263
0.057184	0.08567	0.012287	0.018043	0.273202	0.294183	0.068162	0.073591
0.11316	0.180791	0.02829	0.045152	0.4434	0.666124	0.11085	0.166818
0.202114	0.250518	0.050528	0.056043	0.726401	0.819806	0.1816	0.203059
0.237926	0.292555	0.055083	0.073144	0.80627	1.200069	0.202187	0.300334
0.274464	0.402145	0.068616	0.10063	2.479029	4.001244	0.619757	1.005953
0.572885	0.612758	0.184866	0.304979	9.940853	9.96337	9.891528	9.897158
0.739464	1.21831	0.280766	0.330102	10.13981	10.22441	9.94127	9.962689
1.123063	1.709855	0.317172	0.429211	12.60757	12.89825	12.15272	12.22611
9.935563	9.955609	9.886118	9.891087	13.29878	13.74717	12.3267	12.44246
10.15848	10.23886	9.942226	9.96338	19.73181	34.31511	19.74585	34.49796
10.51006	10.70615	10.03638	10.08487	19.74834	34.53212	19.7498	34.55513
11.81563	12.32114	10.89618	11.02277	24.12728	39.97523	24.03166	39.82066
14.6754	16.17808	12.67426	13.05513	24.1801	42.14375	24.04422	42.03478
19.61033	30.46977	19.70954	30.70883	39.84379	42.45909	39.78458	42.10445
19.67923	33.88756	19.72998	34.36745	60.3192	60.59028	60.07988	60.1484
19.73003	34.08166	19.73805	34.41369	60.70885	61.30539	60.17777	60.33049
19.74112	34.49645	19.74414	34.53471	79.52937	139.0644	79.52963	139.1485
24.05871	37.23607	24.01318	37.91591	120.05	170.1669	120.0125	170.1354
24.47121	39.78031	24.11311	39.55905	120.0653	170.473	120.0162	170.2122
39.55834	40.48271	39.49942	39.991	170.2271	210.2012	170.1505	210.0503
40.08302	42.23185	39.84444	40.86388	170.5218	210.502	170.2243	210.1255
40.57139	42.6491	39.96943	42.00305	340.226	380.3159	340.2439	380.2554
61.66077	63.03005	60.41787	60.78776	340.2746	595.4737	340.256	595.4464
62.79635	64.91327	60.70219	61.25418	380.414	595.6023	380.28	595.4785
78.86084	91.1649	78.94152	91.03431	760.4954	1330.859	760.4767	1330.832

Table A.20 Nonlinear natural frequency when $\upsilon = 0$ and $\upsilon = 0.3$ for $L = 20$ and $L = 40$ of a C–C beam ($a/r = 2.0$)

a/r = 2				*a/r = 2*			
N=6				*N = 4*			
L = 20		*L = 40*		*L = 20*		*L = 40*	
υ=0	υ=0.3	υ=0	υ=0.3	υ=0	υ=0.3	υ=0	υ=0.3
0.00064	0.00096	4.1E-05	6.2E-05	0.00085	0.0012	6.9E-05	9.6E-05
0.00396	0.00571	0.00026	0.00038	0.00576	0.0078	0.00076	0.0009
0.01133	0.0158	0.00077	0.00111	0.02199	0.02925	0.00299	0.00352
0.01637	0.02221	0.00128	0.00192	0.04937	0.07273	0.01234	0.01818
0.04919	0.06884	0.00597	0.00825	0.19774	0.27496	0.04937	0.06829
0.05119	0.07212	0.01229	0.01804	0.27276	0.29402	0.06815	0.07355
0.12146	0.1917	0.02886	0.04594	0.4447	0.66755	0.11091	0.16688
0.2039	0.24991	0.05065	0.05604	0.69951	0.80701	0.1795	0.20235
0.23745	0.29253	0.05507	0.07314	0.83856	1.22309	0.20469	0.30181
0.27547	0.40406	0.06866	0.10073	2.48042	4.00383	0.61985	1.00612
0.57928	0.63291	0.18492	0.30509	9.94085	9.96337	9.89153	9.89716
0.74042	1.22013	0.26427	0.31571	10.1398	10.2244	9.94127	9.96269
1.15354	1.75988	0.34335	0.46067	12.6076	12.8983	12.1527	12.2261
9.93556	9.95561	9.88612	9.89109	13.299	13.7475	12.3267	12.4425
10.1585	10.2389	9.94223	9.96338	19.732	34.3155	19.7459	34.498
10.5101	10.7062	10.0364	10.0849	19.7484	34.5323	19.7498	34.5551
11.8157	12.3216	10.8963	11.0229	24.1281	39.9753	24.0317	39.8207
14.6748	16.1775	12.6742	13.0551	24.1822	42.1451	24.0443	42.0349
19.6122	30.4721	19.7096	30.709	39.8438	42.4626	39.7846	42.1047
19.6799	33.8887	19.7300	34.3675	60.3192	60.5903	60.0799	60.1484
19.7307	34.0821	19.7381	34.4137	60.7089	61.3055	60.1778	60.3305
19.7413	34.4967	19.7442	34.5347	79.5295	139.065	79.5296	139.148
24.0594	37.238	24.0132	37.9161	120.05	170.167	120.013	170.135
24.476	39.7804	24.1134	39.5591	120.066	170.473	120.016	170.212
39.5583	40.4836	39.4994	39.991	170.227	210.202	170.15	210.05
40.083	42.239	39.8444	40.8639	170.522	210.503	170.224	210.126
40.5714	42.6504	39.9694	42.0036	340.226	380.316	340.244	380.255
61.6608	63.0305	60.4179	60.7878	340.275	595.474	340.256	595.446
62.7963	64.9133	60.7022	61.2542	380.414	595.603	380.28	595.479
78.8611	91.1658	78.9415	91.0349	760.495	1330.86	760.477	1330.83